ILMATIETEEN LAITOS
METEOROLOGISKA INSTITUTET
FINNISH METEOROLOGICAL INSTITUTE

128
CONTRIBUTIONS

IDENTIFICATION OF POLLUTION SOURCES AND CHARACTERISTICS OF ATMOSPHERIC COMPOSITION VIA FORWARD AND INVERSE DISPERSION MODELLING

MARJE PRANK

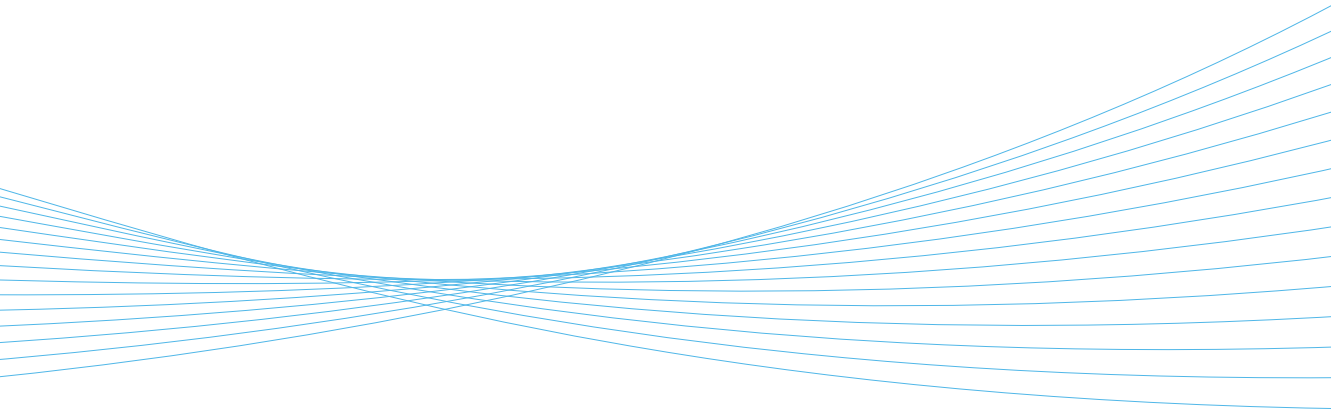

FINNISH METEOROLOGICAL INSTITUTE
CONTRIBUTIONS

No. 128

Identification of pollution sources and characteristics of atmospheric composition via forward and inverse dispersion modelling

Marje Prank

Academic dissertation in Physics

To be presented with the permission of the Faculty of Science of the University of Helsinki, for public criticism in the Auditorium "Brainstorm" of Finnish Meteorological Institute, (Erik Palménin aukio 1, Helsinki) on January 13th, 2017, at 12 o'clock noon.

Finnish Meteorological Institute
Helsinki, 2016

Author's Address: Finnish Meteorological Institute
Atmospheric Composition Research Unit
P.O. BOX 503
FI-00101 Helsinki, Finland
e-mail marje.prank@fmi.fi

Supervisor: Docent Mikhail Sofiev, Ph.D.
Finnish Meteorological Institute

Reviewers: Professor Ole Hertel, Ph.D.
Department of Environmetnal Science
Aarhus Univerity

Carsten Skjøth, Ph.D.
National Pollen and Aerobiology Research Unit
University of Worcester

Opponent: Professor Maria Kanakidou, Ph.D.
Department of Chemistry
University of Crete

Custos: Professor Veli-Matti Kerminen, Ph.D.
Department of Physics
University of Helsinki, Finland

ISBN 978-952-336-004-4 (paperback)
ISSN 0782-6117
Erweko Oy
Helsinki 2016

ISBN 978-952-336-005-1 (pdf)
http://ethesis.helsinki.fi
Helsingin yliopiston verkkojulkaisut

FINNISH METEOROLOGICAL INSTITUTE

Published by
Finnish Meteorological Institute
P.O. Box 503
FI-00101 Helsinki, Finland

Series title, number and report code of publication
Finnish Meteorological Institute
Contributions No. 128, FMI-CONT-128

Date
December 2016

Author
Marje Prank

Title
Identification of pollution sources and characteristics of atmospheric composition via forward and inverse dispersion modelling

Abstract

Atmospheric composition has strong influence on human health, ecosystems and also Earth's climate. Among the atmospheric constituents, particulate matter has been recognized as both a strong climate forcer and a significant risk factor for human health, although the health relevance of the specific aerosol characteristics, such as its chemical composition, is still debated. Clouds and aerosols also contribute the largest uncertainty to the radiative budget estimates for climate projections.

Thus, reliable estimates of emissions and distributions of pollutants are necessary for assessing the future climate and air-quality related health effects. Chemistry-transport models (CTMs) are valuable tools for understanding the processes influencing the atmospheric composition. This thesis consists of a collection of developments and applications of the chemistry-transport model SILAM.

SILAM's ability to reproduce the observed aerosol composition was evaluated and compared with three other commonly used CTM-s in Europe. Compared to the measurements, all models systematically underestimated dry PM_{10} and $PM_{2.5}$ by 10-60%, depending on the model and the season of the year. For majority of the PM chemical components the relative underestimation was smaller than that, exceptions being the carbonaceous particles and mineral dust – species that suffer from relatively small amount of available observational data. The study stressed the necessity for high-quality emissions from wild-land fires and wind-suspended dust, as well as the need for an explicit consideration of aerosol water content in model-measurement comparison. The average water content at laboratory conditions was estimated between 5 and 20% for $PM_{2.5}$ and between 10 and 25% for PM_{10}.

SILAM predictions were used to assess the annual mortality attributable to short-term exposures to vegetation-fire originated $PM_{2.5}$ in different regions in Europe. $PM_{2.5}$ emitted from vegetation fires was found to be a relevant risk factor for public health in Europe, more than 1000 premature deaths per year were attributed to vegetation-fire released $PM_{2.5}$.

CTM predictions critically depend on emission data quality. An error was found in the EMEP anthropogenic emission inventory regarding the SO_x and PM emissions of metallurgy plants on the Kola Peninsula and SILAM was applied to estimate the accuracy of the proposed correction.

Allergenic pollen is arguably the type of aerosol with most widely recognised effect to health. SILAM's ability to predict allergenic pollen was extended to include Ambrosia Artemisiifolia - an invasive weed spreading in Southern Europe, with extremely allergenic pollen capable of inducing rhinoconjuctivitis and asthma in the sensitive individuals even in very low concentrations. The model compares well with the pollen observations and predicts occasional exceedances of allergy relevant thresholds even in areas far from the plants' habitat.

The variations of allergenicity in grass pollen were studied and mapped to the source areas by adjoint computations with SILAM. Due to the high year-to-year variability of the observed pollen potency between the studied years and the sparse observational network, no clear geographic pattern of pollen allergenicity was detected.

Publishing unit
Atmospheric Composition Research

Classification (UDC)
502.3:504.5

638.138:004.942

Keywords
Air quality, aerosols, atmospheric modelling, emission sources
Allergenic pollen, pollen forecasting

ISSN and series title
0782-6117 Finnish Meteorological Institute Contributions

ISBN
978-952-336-004-4 (paperback)
978-952-336-005-1 (pdf)

Language
English

Pages
213

Acknowledgements

I would like to thank Ari Karppinen, who about nine years ago invited me to Finnish Meteorological Institute to work in his group of Air Quality Modelling, and Jaakko Kukkonen for welcoming me to the Air Quality division. I also wish to acknowledge the important role of my supervisor Mikhail Sofiev in introducing me to the world of atmospheric modelling. During these years I have been given a chance to participate in numerous projects and collaborations and I am grateful for the experience. I wish to thank all my colleagues and co-authors with whom I have worked during these years, and especially my closest colleagues from the SILAM group.

I want to thank Professor Hannu Savijärvi for accepting me as a PhD student to Helsinki University and Professor Veli-Matti Kerminen for helping me to finish this path and agreeing to be the Custos.

I am grateful to the official Reviewers of my thesis, Professor Ole Hertel and Carsten Skjoth, for their comments and reviews. I am honoured that Professor Maria Kanakidou has agreed to be the Opponent at the public examination of these thesis.

My sincere gratitude is due to those who have shared this path with me – friends from KFV for making the beginning fun; Joana, Riinu, and Julius for making the end bearable.

I want to thank my family and friends from Tartu who have not forgotten me yet, although many years have passed and our meetings have not always been as frequent as I would have wished.

Helsinki, December 2016,
Marje Prank

Abbreviations

ACM	atmospheric composition model
AMAP	Arctic Monitoring and Assessment Programme
AQMEII	Air Quality Model Evaluation International Initiative
CTM	chemistry-transport model
EAN	European Aeroallergen Network
EC	elemental carbon
ECCAD	Emissions of atmospheric Compounds & Compilation of Ancillary Data
ECMWF	European Center for Medium range Weather Forecasting
ED-3	EuroDelta III
EFI	European Forest Institute
EMEP	Co-operative Programme for monitoring and evaluation of the long-range transmission of air pollutants in Europe
FAC2	fraction of model values that are within a factor of 2 from the observed ones
FRP	Fire Radiative Power
GFAS	Global Fire Assimilation System
GFED	Global Fire Emissions Database
HIALINE	Health Impacts of Airborne Allergen Information Network (EU FP7 funded project)
HIRLAM	HIgh Resolution Limited Area Model
IS4FIRES	Integrated Monitoring and Modelling System for wildland Fires
nss-Ca	non-seasalt calcium

MODIS	Moderate Resolution Imaging Spectro-radiometer
NWP	numerical weather prediction
PM	particulate matter
PM$_x$	particulate matter with an aerodynamic diameter smaller than x μm
SILAM	System for Integrated modeLling of Atmospheric composition
SIA	secondary inorganic aerosol
SOA	secondary organic aerosol
SPI	seasonal pollen index
TRANSPHORM	Transport related Air Pollution and Health impacts - Integrated Methodologies for Assessing Particulate Matter (EU FP7 funded project)
OA	organic aerosol
OC	organic carbon
OM	organic mass
VOC	volatile organic compound

Contents

List of publications

This thesis consist of an introductory review, followed by 5 research articles. Papers I – IV are open access and reproduced under the Creative Commons licence. Papers V is reproduced with the permission of the publisher Elsevier. In the introductory part, these paper are cited according to their roman numerals.

I Prank, M., Sofiev, M., Tsyro, S., Hendriks, C., Semeena, V., Vazhappilly Francis, X., Butler, T., Denier van der Gon, H., Friedrich, R., Hendricks, J., Kong, X., Lawrence, M., Righi, M., Samaras, Z., Sausen, R., Kukkonen, J., Sokhi, R., 2016. Evaluation of the performance of four chemical transport models in predicting the aerosol chemical composition in Europe in 2005. *Atmospheric Chemistry and Physics 16*, 6041–6070. doi:10.5194/acp-16-6041-2016

II Kollanus, V., Prank, M., Gens, A., Soares, J., Vira, J., Kukkonen, J., Sofiev, M., Salonen, R.O., Lanki, T., 2016. Mortality due to vegetation-fire originated $PM_{2.5}$ exposure in Europe – assessment for the years 2005 and 2008. *Environmental Health Perspectives*. doi:10.1289/EHP194

III Prank, M., Sofiev, M., Denier van der Gon, H. a. C., Kaasik, M., Ruuskanen, T.M., Kukkonen, J., 2010. A refinement of the emission data for Kola Peninsula based on inverse dispersion modelling. *Atmospheric Chemistry and Physics 10*, 10849–10865. doi:10.5194/acp-10-10849-2010

IV Prank, M., Chapman, D.S., Bullock, J.M., Belmonte, J., Berger, U., Dahl, A., Jäger, S., Kovtunenko, I., Magyar, D., Niemelä, S., Rantio-Lehtimäki, A., Rodinkova, V., Sauliene, I., Severova, E., Sikoparija, B., Sofiev, M., 2013. An operational model for forecasting ragweed pollen release and dispersion in Europe. *Agricultural and Forest Meteorology 182-183*, 43–53. doi:10.1016/j.agrformet.2013.08.003

V Buters, J., Prank, M., Sofiev, M., Pusch, G., Albertini, R., Annesi-Maesano, I., Antunes, C., Behrendt, H., Berger, U., Brandao, R., Celenk, S., Galan, C., Grewling, L., Jackowiak, B., Kennedy, R., Rantio-Lehtimäki, A., Reese, G., Sauliene, I., Smith, M., Thibaudon, M., Weber, B., Cecchi, L., 2015. Variation of the group 5 grass pollen allergen content of airborne pollen in relation to geographic location and time in season. *Allergy and Clinical Immunology 136*, 87–95. doi:10.1016/j.jaci.2015.01.049

Review of the papers and the author's contribution

Paper I investigates the abilities of four commonly used chemical transport models to reproduce the PM concentration and composition in Europe in 2005. All models are found to substantially underestimate the PM concentrations. The worst represented aerosol components are found to be the carbonaceous and crustal components. Improvements are found necessary also for the wild-land fire emissions.

The author of the thesis performed the modelling with the SILAM model, collected the data from the other modelling groups, planned and performed the analysis of the data, and wrote the paper.

Paper II studies the health effects resulting from the exposure to the smoke from wild land fires in Europe. It was found that the air pollution due to $PM_{2.5}$ released from vegetation fires is a relevant risk factor for public health, especially in Southern and Eastern Europe, although the lower concentrations in western and northern Europe also contributed significantly to the overall attributable mortality.

The author of the thesis performed the modelling to obtain the vegetation fire originated $PM_{2.5}$ concentrations for 2005 and 2008. The 2005 data originated from the same model simulations as used in Paper I. The author also contributed to writing the paper supplying the description of the model simulations and the discussion of the simulation results and their uncertainties, variability, and relevant weather patterns.

Paper III presents a correction for the commonly used EMEP emission inventory for an error found in the emissions of industrial sources on Kola Peninsula. The paper was based on an unexpected finding when modelling the origin of the aerosol peaks measured during a field campaign in Värriö, Finnish Lapland. It was found that the emissions of the metal industry site Nikel were missing in the EMEP inventory and also in other available inventories of anthropogenic emissions in Europe. A corrected emission map was suggested and its accuracy evaluated.

The author of the thesis analysed the emission data from various inventories, performed the forward and adjoint model simulations, analysed the results and was the lead author of the paper.

Paper IV describes the development of the emission model for the pollen of common ragweed (Ambrosia Artemisiifolia L.). An operational model was developed for forecasting the ragweed pollen release and dispersion in Europe.The ragweed-related developments in SILAM concentrated on the formulations of the source term, which supplies the released pollen to the transport and deposition modules. Comparison with the observational data shows that the model reproduces the season propagation and the spatial pattern of total pollen amount fairly well both in the main source regions and further away.

The author of the thesis developed the module for the ragweed pollen emission for SILAM based on available literature, calibrated it with the pollen observations, performed its evaluation and wrote the paper.

Paper V studies the variations in the allergenity of grass pollens (pollen potency). The dependences of the potency on weather conditions and pollen origin are analysed.

The author of the thesis performed the adjoint SILAM model simulations necessary for delineating the pollen origin, contributed to the analysis of the variability of the observed potency and to the writing of the related parts of the paper.

Chapter 1

Introduction

Exposure to airborne particulate matter (PM) has been estimated to be among the ten most significant risk factors for public health globally and among the 15 most relevant for Europe (*Lim et al.*, 2012). It significantly increases the risks of respiratory and heart diseases in both short and long term (*Hänninen et al.*, 2014; *Hansell et al.*, 2015). Recently, air pollution and especially the particulate matter were classified as carcinogenic by WHO (*Loomis et al.*, 2013). *Dai et al.* (2014) concluded that particulate mass alone might not be sufficient to evaluate the health effects of particles. Intensive research efforts have been dedicated to specify the health relevance of specific chemical aerosol components, although the results are this far inconclusive.

Allergenic pollen is arguably the type of aerosol with the most obvious effect to health. Due to raising allergy levels among the European population, the airborne allergenic pollen has become an important part of air quality. *Sofiev and Bergmann* (2013) list the 12 most allergy relevant pollen species in Europe: *Betula* (birch), *Poaceae* (grasses), *Olea* (olive), *Ambrosia* (ragweed), *Alnus* (alder), *Artemisia* (mugwort), *Chenopodiaceae* (goosefoots), *Corylus* (hazel), *Cupressaceae/Taxaceae* (cypresses, yews), *Platanus* (plane tree), *Quercus* (oak) and *Urtica/Parietaria* (wall pellitory, nettle). The pollens of some allergy-relevant species, such as birch and ragweed, are about 20 micrometers or less by diameter and with suitable conditions these can be transported over hundreds or even thousands of kilometers.

In addition to the health effects, particulate matter has been recognized as a strong climate forcer that influences the Earth's energy balance through direct radiative effects and cloud processes. Clouds and aerosols contribute the largest uncertainty to the radiative budget estimates (*IPCC*, 2013; *Khain*, 2009). Both aerosol radiative properties and its hygroscopicity and ability to serve as a cloud condensation nuclei depend critically on its composition.

The substantial effects of atmospheric composition on health and climate make it necessary to monitor and forecast the concentrations of the relevant tracer species. The observational networks cannot cover the whole atmosphere and the observations of a sparse network cannot always be extrapolated to other areas. Remote sensing by satellite-borne instruments can cover large areas, but often with

low temporal resolution. The observations also rarely resolve the vertical profiles of the observed quantities. Thus, the numerical models are often the only feasible source of information about the atmospheric composition.

As both the health and climate effects of aerosols depend on their chemical and physical properties, it is important for the atmospheric chemistry and transport models (CTMs) to accurately assess not only the total amount of PM but also the chemical composition, size spectra and other physical and chemical features of the particles.

The main scientific objectives of this study were:

1. quantifying deficiencies in modelling PM concentration in terms of the aerosol chemical constituents, source categories, seasonal variations, and geographical distribution and identifying the most prominent areas for model improvement;

2. evaluating the health effects of the fine particles originating from wild-land fires;

3. determining the sources and the extent of atmospheric transport of the pollen of common ragweed in Europe;

4. assessing the variability in grass pollen potency (allergen content of a single pollen).

This work is focused on development, evaluation and application of a 3D regional atmospheric chemistry and transport model SILAM. The thesis describes the following developments and improvements of the SILAM model and its input datasets:

1. improving the anthropogenic emission data through a combination of forward and inverse modelling;

2. extending the number of allergenic pollen species in SILAM forecasts;

3. taking the first steps towards modelling the variations of pollen potency by mapping the source areas of grass pollen with different potencies.

Chapter 2

Background

2.1 Atmospheric composition modelling

Atmospheric composition models simulate the concentrations of the tracer compounds in the atmosphere. The models exist in different levels of complexity and work on different spatial and temporal scales, thus the selection of the model depends on the processes of interest in the specific study. Empirical models are based on statistical relations derived from the observations, while the mechanistic ones rely on the mathematical implementation of the current understanding of the chemical and physical processes affecting the studied quantities. The empirical relationships cannot be extrapolated outside the range of the underlying observations, and thus the empirical models are not always valid for assessing the air quality in the future climate or for evaluating the effectiveness of emission abatement measures. In these cases, mechanistic models based on the best understanding of the processes that control the atmospheric composition need to be applied.

This thesis focusses on mechanistic modelling of atmospheric composition in regional scale, with the model domain sizes starting from a few hundreds of kilometres in width, and the most extensive simulations covering the whole European continent. The simulated processes include emission, along-wind transport, turbulent mixing, chemical and physical transformations, and dry and wet deposition of the pollutants. A wide range of methods and parametrizations is used in the various chemistry-transport models (CTMs) for modelling these processes, described for instance by *Kukkonen et al.* (2012).

The model input consists of the emissions of the tracers and the meteorological fields from numerical weather forecasting (NWP) models. The NWP models and CTMs can either work off-line or be on-line coupled, depending on whether there is two-way data exchange between the models during the computation or whether the output of the NWP model is just read by the CTM as input. In the Lagrangian framework, the transport of discreet air parcels is described as a random-walk process, while the Eulerian models compute the evolution of the concentrations in a 3D grid. The model output usually consists of temporarily resolved gridded 3D tracer concentration and 2D deposition fields.

2.1.1 Adjoint modelling, footprints

Back trajectory analysis is a widely used method for investigating the origin of the observed tracer concentrations (*Stein et al.*, 2015). Also a more quantitative method – the footprint analysis, which is based on solving the adjoint transport and transformation equations – has been applied for tracing the origin of the observed air-masses, for instance by (*Stohl et al.*, 2002) using a Lagrangian and (*Hourdin and Talagrand*, 2006) using an Eulerian models. Such receptor oriented modelling, where the model starts from the observed state and the computation goes backwards in time allows computing the sensitivity of the observation to model parameters and input. For instance, the observed pollutants can be traced back to their sources and as the adjoint model allows to compute the sensitivity of the observation to the emission fluxes from every point of the model domain, it can be used to estimate the source properties (*Shankar Rao*, 2007; *Pudykiewicz*, 1998; *Flesch et al.*, 1995). The footprint of the observation comprises the non-zero values of the sensitivity distribution and the emissions from this area are responsible for the observed concentration.

2.1.2 Modelling the aerosol composition

Atmospheric aerosols consist of a mixture of primary and secondary compounds of both natural and anthropogenic origin. Sizes of aerosol particles range from a few nanometres to several tens of micrometers. Most of the mass of tropospheric aerosols consists of sulphate, ammonium, nitrate, sodium and chloride ions, elemental and organic carbon, crustal elements, and water. The particle size and composition can change due to chemical reactions or aerosol processes such as coagulation, condensation or evaporation, which lead to each particle having a unique composition. Exhaustive studies about aerosol composition in Europe have been published by *Belis et al.* (2013), *Van Dingenen et al.* (2004) and *Putaud et al.* (2004b, 2010), who report that the $PM_{2.5}$ fraction is dominated by secondary inorganic aerosol (SIA) and carbonaceous particles, while the coarse fraction ($PM_{2.5-10}$) includes large contributions from mineral dust and also sea salt at coastal stations. Nitrates are still noticeable in coarse PM, while ammonium and sulphate contribute on average just by a few percent to the coarse fraction. Secondary organic aerosol (SOA) makes up majority of organic carbon, especially in rural stations and during warm periods (*Belis et al.*, 2013), indicating an important role of the biogenic emissions of the volatile organic compounds (VOCs). Significant contributions from biomass burning can be observed during cold season indicating domestic heating. In Central Europe carbonaceous matter contributes noticeably also to coarse particles and generally there is more carbonaceous matter in Central Europe, more nitrate in North-western Europe, and more mineral dust in southern Europe (*Putaud et al.*, 2004b, 2010).

Due to the impact of aerosols on climate and health, it is important for the atmospheric chemistry and transport models to accurately assess not only the total PM amount but also the particle chemical composition, size spectra and other physical and chemical features.

Particulate matter consists of both primary components directly emitted in

particulate phase and secondary components that form by chemical and physical processes in atmosphere. A substantial proportion of secondary aerosols consists of components, such as ammonium nitrate and semi-volatile organic species, whose partitioning between gaseous and particulate phase depends on the atmospheric conditions and concentrations of the compounds. The models use a range of different algorithms for assessing this equilibrium, such as the thermodynamic equilibrium model ISORROPIA (*Nenes et al.*, 1998) for the inorganic components and water or the Volatility Basis Set (VBS, (*Donahue et al.*, 2006)) for the partitioning of the organic components.

Modelling studies often report underestimation of total PM mass concentration (*Im et al.*, 2014; *Solazzo et al.*, 2012a; *Stern et al.*, 2008, etc.). This underestimation (also called PM deficit) is often easy to accept, because the models rarely include all the aerosol components. For instance, secondary organic aerosols, forest fire induced aerosols and wind-suspended dust are often left out because of limited knowledge of their emissions or production in the atmosphere (*Kukkonen et al.*, 2012). Uncertainties in SOA modelling are described for instance by *Bergström et al.* (2012), fire emission uncertainties by *Soares et al.* (2015), dust emission uncertainties by *Kim et al.* (2014).

The properties of hygroscopic aerosols depend strongly on ambient relative humidity – the particles in the atmosphere gain and lose water depending on their hygroscopic properties and the available water vapour. This process influences the aerosol size distribution, which in turn affects both dry and wet deposition, and also the optical properties of the particles and their interaction with solar radiation. Hysteresis exists in the particle deliquescence-crystallization cycle for many aerosol components – the deliquescence humidity, at which the dry solid particle starts taking up water is significantly higher than the efflorescence humidity, at which the particle crystallizes and loses its water content. The deliquescence and efflorescence humidities differ for external and internal mixtures of different inorganic salts (*Seinfeld and Pandis*, 2006; *Martin*, 2000) and also the presence of organic components in the same particles can alter the water uptake of the inorganic species (*Jing et al.*, 2015). This makes modelling the aerosol water content challenging, because the water uptake depends on the aerosol composition and mixing state of the different components, but also on whether the particle comes from more or less humid environment.

2.1.3 Allergenic pollen modelling

A pollen of a wind pollinated plant is usually a large and light particle, with diameter in the range of a few tens of micrometers, and modelling its transport and deposition is feasible with a regular CTM, as shown by *Sofiev et al.* (2006a). The first studies about modelling pollen dispersion in Europe were published about 10 years ago (*Helbig et al.*, 2004; *Vogel et al.*, 2008; *Schueler et al.*, 2005; *Schueler and Schlünzen*, 2006; *Sofiev et al.*, 2006a; *Siljamo et al.*, 2008). During the last decade, pollen dispersion has been incorporated into numerous reginonal CTMs (COSMO (*Helbig et al.*, 2004; *Vogel et al.*, 2008; *Zink et al.*, 2012), Enviro-HIRLAM (*Mahura et al.*, 2009), CHIMERE and RegCM (*Hamaoui-Laguel et al.*, 2015),

CMAQ, (*Zhang et al.*, 2014), etc). In the SILAM CTM currently the pollen emission models exist for birch (*Sofiev et al.*, 2013; *Siljamo et al.*, 2013), grasses, olive, alder, mugwort (*Prank et al.*, 2016) and ragweed (**Paper IV**). The SILAM birch pollen source term was recently used in the first study about ensemble modelling of pollen dispersion (*Sofiev et al.*, 2015a).

Also the biogenic emission models have started modelling pollen emission for various plant species (LPJ-Guess (*Leiblein-Wild et al.*, 2015), MEGAN (*Zhang et al.*, 2014)).

A pollen emission model for regional simulations requires two main components: a habitat map and a flowering model specifying the dependencies of the season timing on external forcings. As one of the main reasons for modelling pollen with a regional CTM is to forecast the long-range transport episodes originating occasionally from hundreds, or even thousands of kilometers away, all maps and parametrizations have to be valid for the whole computed region.

Several data sources exist for plant habitat maps. Land cover and forest inventories can contain either the required land use type (e.g. alder or birch forests, olive plantations or grasslands) or a surrogate type that needs to be scaled for the specific species (e.g. broadleaf forest for birch or alder). Possible data sources include detailed databases, such the Global Biodiversity Information Facility (GBIF, www.gbif.org) that provides the data on observations of specific plant species or European Forest Institute's (EFI) database on tree species (*Brus et al.*, 2012). However, such sources have not proved to be very useful, as the observation practices differ noticeably between regions (*Cunze et al.*, 2013), leading to unrealistically uneven habitat maps, and low accuracy in reproducing the forest composition (*Trombik and Hlásny*, 2013). For the invasive ragweed, detailed maps have been compiled for some of the most affected regions (Pannonian plain, *Skjøth et al.* (2010); France, *Thibaudon et al.* (2014); Austria, *Karrer et al.* (2015)) based on land use, topography and local knowledge. Unfortunately these maps do not cover the whole Europe. Thus, the more general land-cover maps often have to be used for starting points, and the habitat maps have to be obtained by calibrating those with the pollen observations. For example, the broadleaf forest map of EFI (*Päivinen et al.*, 2001; *Schuck et al.*, 2002) was used in SILAM for birch and alder habitats. However, also the quality of the available land cover data has been criticised by *Fritz et al.* (2011).

The timing and intensity of the flowering season of a plant species varies both geographically and from year to year. For annuals, the intensity of the flowering season depends on the suitability of the meteorological conditions and availability of resources (water, nutrients, solar radiation) during the growing season, while for perennial plants, two or three year cycles are often observed in the flowering intensity (*Dahl et al.*, 2013). Various forms of competitions for resources between the ripening of the seeds and the preparations for the next year's reproductive efforts have been suggested as an explanation, with spatial synchronization imposed by the interannual variations in the environmental conditions (*Dahl et al.*, 2013).

The onset and duration of the flowering can be influenced by meteorological and physical parameters such as temperature, photoperiod, and availability of resources (e.g. water, nutrients, CO_2). In annuals, such as ragweed, mugwort and some

grasses, the photoperiod often plays important role, modulated to varying extent with temperature and water availability (*Dahl et al.*, 2013; *Grewling et al.*, 2012). For trees, various types of temperature accumulation models are commonly used for predicting the phenological phases (e.g. *Linkosalo et al.* (2006); *Andersen* (1991); *Galan et al.* (2005)). Additionally, many tree species (including birch, olive, and alder) have a "chilling requirement" – to avoid frost damage by too early initiation of flowering, they require a certain period of low temperatures before the winter dormancy can be lifted (*Dahl et al.*, 2013; *Orlandi et al.*, 2004).

The temporal profile of the observed pollen season of a taxon can have several peaks (e.g. *Spieksma et al.* (1989); *Grewling et al.* (2012)). One reason for that can be that the pollen originates from areas with substantially different microclimates, which can happen in mountainous or seaside regions. Multi-peak seasons can also occur if several species with different phenological requirements contribute to the same pollen observations. This complicates the modelling of the duration of the pollen season. However, the accuracy of the forecasts of season end is much less relevant for the allergy patients than the accuracy of predicting the start of the season, in order to start the medications in time.

The calibration of the flowering model would ideally be based on phenological observations. The observations of the timing of the phenological phases for many species are available from the Pan European Phenology Project website (http://www.pep725.eu). While for some species (e.g. birch, alder) a large dataset about the start of flowering is available, for many other species, such as mugwort and ragweed, the data is available only from one or two countries, which is not sufficient to capture the behaviour over whole Europe. Very few observations exist in the database about the end of flowering. Thus, often the pollen observations have to be used for the calibration of the phenological model. However, *Estrella et al.* (2006) found significant differences, when comparing the season propagation in the pollen observations with the observations of local flowering.

Due to the fact that the pollen observations are rarely publicly available, the opportunities for evaluating the pollen emission models are limited. For example, *Zhang et al.* (2014) compare their modelling results with only one year of observations in 9 stations, and *Leiblein-Wild et al.* (2015) report only visual comparison with the graphic maps available at the website of the European Aeroallergen Network (EAN, https://www.polleninfo.org).

Pollen grains, when inhaled, release a mixture of proteins, some of which can cause an allergic response in the sensitive individuals. As shown by *Buters et al.* (2012); *Galan et al.* (2013) and **Paper V**, the allergen released from the same amount of pollen varies substantially between the measurement stations and also from day to day in the same location, depending on the meteorological conditions and the area of origin of the pollen. Thus, although the airborne pollen observations are a good proxy for allergen exposure, more can be learned from the actual monitoring and modelling of allergens in ambient air.

2.2 Model evaluation

To gain trust in the model, its predictions need to be compared with the available observations. Model evaluation can serve several goals: determine the model's suitability for a given task, understand the strengths and limitations of different models, and guide the model improvement (*Dennis et al.*, 2010). Numerous publications compare the results of a single model to a set of observations, using the range of methodologies described in *Dennis et al.* (2010). However, for such study the modeller is free to select the set of observations and the statistical scores of the model skill to be presented, and to choose the best model set-up to reproduce the selected observations. As these choices are not the same between different studies, the skills of the models are usually not directly comparable, ant thus these studies do not give an objective picture of how the presented model or models in general manage in all conditions. Multi-model intercomparison studies provide a more objective view, as all the models are compared to the same set of observations in an identical way, and often the model input data is also unified.

Such intercomparison studies for atmospheric composition modelling have been made in many projects, e.g. AEROCOM (*Textor et al.*, 2006) for global models, and HTAP (*Dentener et al.*, 2010) for hemispheric modelling. For Europe numerous studies can be mentioned, such as EUROTRAC (*Hass et al.*, 1997, 2003), AQMEII (*Rao et al.*, 2011; *Solazzo et al.*, 2012a,b; *Im et al.*, 2014), MACC (*Huijnen et al.*, 2010b; *Marécal et al.*, 2015), EURO/CITYDELTA (*Vautard et al.*, 2007, 2009; *Bessagnet et al.*, 2014), ENSCLIM (*Langner et al.*, 2012; *Simpson et al.*, 2014; *Soares et al.*, 2016) and others.

It has also become increasingly common in projects studying either future climate scenarios or the effects of emission control measures to apply several models of the same type, obtaining an ensemble of the predictions (*Dentener et al.*, 2010; *Langner et al.*, 2012; *Simpson et al.*, 2014; *Colette et al.*, 2015; *Soares et al.*, 2016), etc. This is a way to improve the robustness and reproducibility of the scenario results that cannot be validated against observations, showing that models with different algorithms and assumptions show a similar response to the changes in the model forcings.

A specific challenge of the model-measurement comparison for individual PM components is the difference in how PM composition is represented in the models and observations. The observations are available for specific molecules or ions (Na^+, SO_4^{2-}, NH_4^+, NO_3^-, Ca^{2+}, Al, Fe, etc.) and elemental and organic carbon (EC, OC), while in the models the speciation of primary aerosols rather follows the emission categories, such as anthropogenic sources, wild-land fires, sea salt or wind-blown dust, which all can include several of the measured components.

As a further complication, the PM speciation measurements do not resolve the whole PM mass. Observational studies of the PM mass closure (*Putaud et al.*, 2004a; *Sillanpää et al.*, 2006) have reported an unidentified fraction of fine PM reaching up to 20-30% of the gravimetrically determined aerosol mass, while it might be as large as 40% for coarse particles. The explanations for this deficiency include possible artefacts in observations of semivolatile organic and inorganic components, unaccounted non-carbon atoms (e.g. O, H) in organic matter, uncertain-

ties in estimating the concentration of the crustal particles, and most importantly aerosol-bound water.

In gravimetric sampling, which is the reference method for PM observations defined by the European Committee of Standardization, the filters are weighted in laboratory conditions of 20° C and 50% relative humidity. While the deliquescence relative humidity of most pure inorganic salts present in the atmospheric aerosol is higher than 50% (*Martin*, 2000), it can be lower for mixed particles (*Seinfeld and Pandis*, 2006). The efflorescence humidity is below 50% for many common aerosol components, such as ammonium sulphate and sodium chloride (*Martin*, 2000). Therefore, if the particle has been exposed to a more humid outdoor environment, crystallization might not occur in the standard laboratory conditions, leaving some water bound to the particles on the filter. However, the output of the chemistry-transport models usually consists of dry particulate matter concentrations.

The spatial features of the compared data can also lead to uncertainties when comparing the model grid-cell average with concentration observed in a single point. Regional models with grid-cell sizes of a few tens of kilometres are not designed to reproduce the concentration patterns with smaller spatial scales, e.g. in the vicinity of strong sources, in urban conditions or mountainous areas. Also the vertical gradients can be steep in the concentrations of surface emitted or fast depositing pollutants and introduce extra uncertainties to the model evaluation against surface or roof level observations.

2.3 Health impact of fine particulate matter

Adverse health effects arising from fine PM are well recognized (*Lim et al.*, 2012; *Hänninen et al.*, 2014; *Hansell et al.*, 2015; *Loomis et al.*, 2013). As the toxicity of the inhaled aerosol depends on its chemical composition, intensive research efforts have been dedicated to specify the health relevance of specific aerosol components, although the results are still inconclusive. Several epidemiological studies relate the strongest adverse health outcomes with sulphate and crustal aerosols, and carbonaceous aerosols originating from combustion sources including traffic (*Stanek et al.*, 2011; *Dai et al.*, 2014; *Ostro et al.*, 2011; *Zanobetti et al.*, 2014; *Atkinson et al.*, 2015), while no PM components have been unequivocally proven to have zero health impact (*Rohr and Wyzga*, 2012). Toxicological studies, on the other hand, have not shown direct toxicity of the secondary inorganic salts, elemental carbon, crustal dust, and sea salt in ambient concentrations, indicating complex interactive effects with other pollutants (*Schlesinger and Cassee*, 2003; *Schlesinger*, 2007; *Cassee et al.*, 2013). The toxicity of wood smoke has been found to vary depending on burning conditions (*Cassee et al.*, 2013). Due to these complications, majority of the health impact assessments still concentrate on total mass of fine PM.

Chapter 3

Models and data

3.1 SILAM chemistry-transport model

The thesis presents a collection of developments and applications of the System for Integrated modeLling of Atmospheric coMposition (SILAM, http://silam.fmi.fi). SILAM is a global-to-meso-scale chemical transport model developed at Finnish Meteorological Institute and used in research and operational applications related to air quality and emergency. SILAM can be used with two transport algorithms - the Eulerian advection scheme of *Sofiev et al.* (2015b), and the Lagrangian advection scheme described by *Sofiev et al.* (2006b). Adjoint models exist for both Lagrangian and Eulerian advection mechanisms.

SILAM includes a meteorological pre-processor for diagnosing the basic features of the boundary layer and the free troposphere from the meteorological fields provided by various meteorological models (*Sofiev et al.*, 2010). The dry deposition scheme is described in *Kouznetsov and Sofiev* (2012).

Several options exist in SILAM for atmospheric chemistry, between which the user can choose. The gas phase chemistry can be simulated by the Acid-Basic scheme from DMAT model (*Sofiev*, 2000), or the Carbon Bond Mechanism IV (CBM-IV, *Gery et al.* (1989)) can be used with reaction rates updated according to the recommendations of IUPAC (http://iupac.pole-ether.fr) and JPL (http://jpldataeval.jpl.nasa.gov) and with several possible alternations, such as either including the stratospheric chlorine reactions or the terpenes oxidation from CB05 reaction list (*Yarwood et al.*, 2005). A linear chemistry scheme for the sulphur oxides is also available (*Sofiev*, 2000).

Flexible options exist for the aerosol representation. The possible aerosol components in SILAM include primary particulate matter, either as total or speciated to multiple components, secondary inorganic species SO_4^{2-}, NO_3^- and NH_4^+, fresh and aged elemental carbon, primary and secondary organic carbon, desert dust, sea salt, smoke from wild-land fires and allergenic pollen.

For secondary inorganic aerosol formation, an updated version of the chemistry scheme from DMAT model (*Sofiev*, 2000) is used. It includes gas phase and heterogeneous oxidation of SO_2 to SO_4, dynamic equilibrium between NH_4NO_3 aerosol

and NH_3 and HNO_3 in gas phase. The scheme has been extended by including the formation of coarse nitrates by the condensation of HNO_3 to the surface of the sea salt particles.

A volatility basis-set (VBS) scheme (*Donahue et al.*, 2006; *Robinson et al.*, 2007) is implemented in SILAM for modelling the secondary organic aerosols (SOA). The SOA production is computed from toluene, xylene, isoprene and monoterpenes. NOx-dependent SOA yields of *Lane et al.* (2008) are used. VBS in SILAM has one non-volatile bin and four semivolatile bins (1-1000 μg m^{-3} saturation concentrations), separately for SOA from biogenic and anthropogenic precursors. Three intermediate volatility (IVOC) bins (1e4 - 1e6 μg m^{-3}) have been added for anthropogenic OC emissions, for which the volatility distributions from e.g. *Shrivastava et al.* (2008, 2011) can be used. The scheme is implemented keeping in mind various test purposes, thus the OH reaction rates of the volatility bins can be defined by the user, separately for biogenic and anthropogenic bins and anthropogenic IVOCs.

Some of the transformation schemes (linear sulphur chemistry, CBM-IV gas phase chemistry, and passive self-decay) can be used in adjoint computations.

Sea-salt is emitted according to *Sofiev et al.* (2011); *Soares et al.* (2016). SILAM uses the biogenic VOC emissions of *Poupkou et al.* (2010), the module is capable of emitting isoprene and monoterpenes. Wild land fire emissions of IS4FIRES v1 *Sofiev et al.* (2009) or v2 *Soares et al.* (2015) can be used, further described below in Section 3.3.2.

Pollen emission can be computed for birch (*Sofiev et al.*, 2013; *Siljamo et al.*, 2013), grasses, olive, ragweed (**Paper IV**), alder and mugwort (*Prank et al.*, 2016) pollens. Further details of pollen emission in SILAM can be found below in the Section 3.3.2.

SILAM includes 3D- and 4D-VAR (*Vira and Sofiev*, 2012) and EnKF schemes for data assimilation.

The SILAM model has been evaluated against other models and air quality and pollen observations over Europe in several recent multi-model inter-comparison studies (*Huijnen et al.*, 2010a; *Solazzo et al.*, 2012a,b, 2013; *Sofiev et al.*, 2015a; *Marécal et al.*, 2015; *Soares et al.*, 2016) and **Paper I**.

3.2 Thermodynamic equilibrium model ISORROPIA2

In **Paper I** the aerosol water content at the filter weighting conditions was evaluated based on the modelled and observed dry PM composition using the thermodynamic equilibrium model ISORROPIA2 (*Fountoukis and Nenes*, 2007). ISORROPIA2 considers the equilibrium between the gas phase NH_3, HCl, HNO_3, H_2SO_4 and aerosol phase Na, Ca, K, Mg, NH_4, NO_3, SO_4 and Cl. It allows to compute the water uptake for stable and metastable states, corresponding to the lower and upper branches of the deliquescence hysteresis loop. In **Paper I**, ISORROPIA2 was run in the reverse mode, where the input quantities were the soluble inorganic components (SIA, sea salt, nss-Ca) in the aerosol phase. Both stable and metastable states were computed, providing the lower and upper limits of the aerosol bound

water amount.

3.3 Emission data

3.3.1 Anthropogenic emission inventories

The inventories of the anthropogenic emissions commonly consist of gridded maps of annual or monthly total emissions by species and are often segregated by the emission sector (industry, traffic, agriculture etc). Different temporal variations and emission vertical profiles are applied in different models (e.g. *Simpson et al.*, 2012; *Bieser et al.*, 2011), which provide the seasonal and diurnal changes in emission intensity and release height of the pollutants depending on the emission sector.

In Europe the emissions of acidifying air pollutants, heavy metals, particulate matter and photochemical oxidants are reported to EMEP (Co-operative Programme for Monitoring and Evaluation of the Long-range Transmission of Air Pollutants in Europe, http://www.emep.int/). Based on these emissions reported officially by the authorities of the countries CEIP (the EMEP Centre on Emission Inventories and Projections) prepares emission inventories for dispersion model input. The inventory includes anthropogenic emissions and some natural sources (volcanoes in Italy and DMS marine fluxes), with yearly time step and 50km spatial resolution. Currently the resolution is about to rise to 0.1 degrees.

There are numerous other inventories of anthropogenic emission, covering various regions and time periods with different spatial and temporal resolutions and containing different sets of pollutant species. The most comprehensive collection of emission data can be found at the website of the ECCAD project (Emissions of atmospheric Compounds & Compilation of Ancillary Data, http://eccad.sedoo.fr). The portal provides access to numerous regional and global datasets of anthropogenic, biogenic, oceanic and biomass burning emissions for various periods. For Europe, the emission inventories currently available with spatial resolution suitable for regional scale modelling are various versions originating from TNO (*Visschedijk et al.*, 2007; *Denier van der Gon et al.*, 2014; *Kuenen et al.*, 2014), and EDGAR (http://edgar.jrc.ec.europa.eu; *Crippa et al.*, 2016).

As shown by *McLinden et al.* (2016), numerous large sources of SO_2 are currently missing in the commonly used emission inventories. **Paper III** reports such error found in the emission database of EMEP. When new emissions patterns are reported by the countries, updated data are reported also for the past years and all emissions are recomputed retrospectively by CEIP. This can result in substantial changes in the emission amounts and patterns. In **Paper III** the EMEP dataset for 2003, downloaded before 2006, was used as the starting point for the analysis.

Other inventories are partly independent from the EMEP database but can sometimes rely on the data reported to EMEP. For instance in the TNO-GEMS inventory for 2003 (*Visschedijk et al.*, 2007), used in **Paper III**, the initial EMEP emission distributions were significantly rearranged but the national totals for most countries were based on the values reported to EMEP. Independent bottom-up assessment from activity data and emission factors was used only if the reported data were missing or suspected to be erroneous.

3.3.2 Natural emissions

If the emission intensity from a source depends on meteorological conditions, the emissions are usually computed on-line within the chemistry-transport model. The emissions of wind-suspended dust and sea salt depend strongly on wind speed, sea salt emissions also depend on water temperature and salinity and dust emissions on soil water content, vegetation and soil properties. Biogenic emissions of VOC-s depend on solar radiation and temperature and the phenological state of the vegetation. Biogenic particulate emissions, such as pollens, fungal spores and plant debris, also follow the phenological developments. The two sets of natural emissions relevant for this study – wild-land fires and allergenic pollen – are described in detail below.

The emissions from wild-land fires

The emissions from wild-land fires can be estimated from satellite observations of either burnt area scars or active fires, such as the Fire Radiative Power (FRP). The first of these approaches is taken for instance in the Global Fire Emissions Database (GFED, *van der Werf et al.* (2010), while the Global Fire Assimilation System (GFAS *Kaiser et al.* (2012) and the Integrated Monitoring and Modelling System for wild-land fires (IS4FIRES) *Sofiev et al.* (2009); *Soares et al.* (2015)) follow the second approach, as it allows near-real-time retrieval of the emission fluxes necessary for air quality forecasting. IS4FIRES emissions used in **Paper I** and **Paper II** are computed using the FRP observations of the Moderate Resolution Imaging Spectro-radiometer (MODIS) on-board Terra and Aqua satellites. Land-use dependent emission factors are used to convert the observed FRP to PM emissions. As MODIS covers every location on the globe at least twice per day, the emissions are computed with daily resolution and a fixed diurnal variation profile is assumed for the emission intensity (*Soares et al.*, 2015). Also a fixed vertical emission profile can be assumed (e.g. uniform distribution up to 1 km in IS4FIRES v1), or the plume rise can be computed for every fire separately based on the observed FRP and the meteorological conditions at the fire location (*Sofiev et al.*, 2012). The latter option was used in SILAM computations presented in **Paper I** and **Paper II**.

Pollen emission modelling

SILAM can compute pollen emission for birch (*Sofiev et al.*, 2013; *Siljamo et al.*, 2013), grasses, olive, alder and mugwort (*Prank et al.*, 2016) pollens. **Paper IV** describes the development of the emission model for common ragweed (*Ambrosia artemisiifolia* L.).

The trees (birch ,olive, alder) are represented as temperature sum dependent species, while the flowering of the annuals such as ragweed, mugwort and grasses has been assumed to mainly depend on photoperiod and thus fixed calendar days can be used as start and end of the flowering season. SILAM allows the parameters of the flowering model to vary spatially, and thus a map of flowering thresholds (temperature sums or calendar days) is necessary for model input.

The temperature sum model for birch pollen emission in SILAM is described by (*Sofiev et al.*, 2013; *Siljamo et al.*, 2013). Broadleaf forest map from EFI (*Päivinen et al.*, 2001) was calibrated with the EAN pollen observations to obtain the habitat map. For grasses the grassland map from ECOCLIMAP database (*Champeaux et al.*, 2005) is used. As the numerous grass species that contribute to the grass pollen have different requirements for flowering onset, and their abundance and flowering intensity varies both spatially and year to year, the grass flowering model in SILAM is based on observed average dates and larger model uncertainties have to be accepted. The olive groves from ECOCLIMAP are used as olive habitat and a similar temperature sum model as used for birch was calibrated using EAN observations. The initial guess for the flowering parameters of alder was taken following the simple degree hour model of (*Andersen*, 1991) – SILAM does not include chill accumulation. The start and ending dates of mugwort flowering were taken from long term averages of EAN observations that were interpolated over whole Europe. As mugwort is mostly found at roadsides, waste areas and other areas with disturbed soil and rarely occurs on crop fields (*Barney and Ditommaso*, 2003), human influenced land uses (roads, inhabited areas, etc.) from ECOCLIMAP land cover (*Champeaux et al.*, 2005) were taken as a first guess for mugwort habitat. These land cover maps were calibrated with the alder and mugwort pollen observations of EAN to obtain the pollen emission maps of these species (*Prank et al.*, 2016).

Common ragweed is a highly allergenic invasive weed, which is spreading through southern and central Europe. Ragweed pollens are relatively small – *Taramarcaz et al.* (2005) reports 18-22 μm diameter, even smaller size (13-15 μm) was reported by *Fumanal et al.* (2007) – and thus can be transported over the whole Europe. Due to the extremely high allergenicity, even small pollen concentrations in the air can cause symptoms in the sensitive population (*de Weger et al.*, 2013). Recently *Grewling et al.* (2016) proved that the long range transported ragweed pollens remain immunoreactive, and thus the long-rage transport episodes can result in adverse health effects.

Ragweed is the only species in SILAM for which the source term utilizes occupancy and climatic habitat quality maps from an ecological model. The ecological model of *Chapman et al.* (2016) was applied to simulate the invasion of Ambrosia Artemisiifolia in Europe, accounting for the climate suitability (temperature during the vegetative season, annual variations in temperature to break the dormancy, available moisture, etc.), seed import from infested areas, seed dispersal from invaded areas, and suitability of land use for ragweed. Both the underlying model and the ragweed habitat map are described by *Bullock et al.* (2012); *Chapman et al.* (2014, 2016). The habitat maps were provided with spatial resolution of 5 x 5 km and further refined based on the comparison of SILAM simulations with EAN observations (**Paper IV**). A multi-threshold model for ragweed flowering was developed in **Paper IV**, based on *Deen et al.* (1998). The flowering was assumed to start when photoperiod gets shorter than 14.5 hours after midsummer, and 25 biodays of *Deen et al.* (1998) are accumulated. The flowering in the model ends when photoperiod shortens to 12 hours, daily mean temperature falls below 7.5 °C or frosts occur.

3.4 Observational data

3.4.1 EMEP opservational network

The observations by the EMEP monitoring network are used in **Paper I** and **Paper III**. Chemical Co-ordinating Centre of EMEP (CCC) aims at long-term monitoring of concentrations and deposition fluxes of air pollution with adequate spatial coverage over Europe. The stations of the EMEP observational network have been chosen to be representative of regional background and thus suitable for comparison with regional models that have grid cell size of a few tens of kilometres (*EMEP*, 2001). Gravimetric sampling is the reference method for PM observations defined by the European Committee of Standardization. Before weighting the filters are equilibrated at 20°C and 50% relative humidity for 48 hours.

Model measurement comparison for aerosol composition

In order to evaluate the model results against the observations, the model output needs to be converted to the observed quantities.

In **Paper I**, the observed Na^+ was assumed to originate only from sea salt, consisting 30.8% of sodium by dry weight. The part of the Ca^{2+} observations not related to sea salt (nss-Ca) was used to evaluate the modelled mineral aerosol. The sea salt related calcium was subtracted from the observations proportionally to observed Na^+ concentrations, sea salt including 1.2% of calcium by dry weight. Widely varying calcium contents have been reported for Saharan dust from different origin areas ranging from <5% to >15% (*Avila et al.*, 1998; *Formenti et al.*, 2011; *Marconi et al.*, 2014; *Putaud et al.*, 2004a). The calcium content of anthropogenic emissions also varies between the sources, ranging from less than a percent for biomass burning (*Akagi et al.*, 2011; *Larson and Koenig*, 1993) to 30% for cement and lime production](*Lee et al.*, 1999; *van Loon et al.*, 2005). In **Paper I** the modelled dust was assumed to come mainly from Sahara and was attributed 10% Ca^{2+} content (*Marconi et al.*, 2014). In addition, 3.5% Ca^{2+} content was attributed to the mineral part of primary anthropogenic emissions. This value was chosen as it maximized the correlation between the observed nss-Ca and the model results. It stays well within the reported range for the anthropogenic emissions. The simulated nss-Ca concentrations were estimated as the sum of the 10% of dust concentrations plus 3.5% of the unspeciated other primary PM concentrations.

The OC to OM ratios have been reported to range from 1.2 to 1.6 for fresh anthropogenic emissions, while factors around 2 have been found for aged, secondary and oxygenated aerosol and particles originating from biomass burning (*Aiken et al.*, 2008; *Turpin and Lim*, 2001). Factor 1.6 was used in this study, analogously to (*Bessagnet et al.*, 2014), however, this might be an underestimation for the EMEP stations, which are mostly located in rural areas and would thus be largely influenced by aged aerosols.

The aerosols emitted by wild-land fires also consist mainly of carbonaceous compounds. The fire emissions originated from IS4FIRES, which provides unspeciated PM_{10} and $PM_{2.5}$ emissions. The fire-emitted PM has been further speciated as post-processing following *Akagi et al.* (2011); *Andreae and Merlet* (2001). On

average these papers suggest roughly 5% EC and 50% OC content for fire emitted aerosol, the rest mainly consisting of non-carbon atoms in the organic compounds and some inorganics (up to 5%).

3.4.2 Observations of pollen and allergen

Majority of pollen air-concentration measurements in Europe are made with Hirst-type volumetric samplers (*Hirst*, 1952). The air is sucked in through a nozzle aimed at a slowly rotating drum, and the airborne particles are deposited on a sticky tape, which is later analysed under a microscope by an aerobiologist, who counts the pollens of different taxa.

The pollen observations in Europe are made by wide range of institutions in different countries. The observational data are collected by European Aeroallergen Network (EAN, https://ean.polleninfo.eu/Ean), who gather the data from a few hundred individual stations to a common database. The EAN archives include pollen counts starting from 1974. For recent years Europe is covered with ∼400 stations. The network covers well the Central Europe, however, it has very limited coverage of the Eastern Europe. The data are not publicly available, and EAN membership and permission from all data owners is necessary for accessing the database and using the data (https://ean.polleninfo.eu/Ean/datausepolicy).

The EAN database includes the pollen counts of numerous different plant taxa. The pollens of different species are not always distinguishable, and thus one pollen taxon can include the pollen from several plant species. For instance, pollens of different grasses can not be distinguished visually and thus all grasses are reported together as single taxon. The ragweed pollen observations of the EAN network are used in **Paper IV**.

Within the HIALINE project *Buters et al.* (2012, 2015); *Galan et al.* (2013) the aerosol samples collected daily for three years with a high-volume cascade impactor from 10 sites in Europe were analysed for the content of the major allergens from birch (Bet v 1), olive (Ole e 1) and grass (Phl p 5) pollen. The allergen levels were determined in two aerosol fractions: $PM_{2.5-10}$ and larger particulates (grass pollen is about 40 μm in diameter, olive about 30 and birch about 20). The allergen measurements were accompanied with pollen observations at the same sites. **Paper V** studies the relations between the grass pollen and allergen concentrations in air and the variations in their ratio - the pollen potency.

3.5 Model setup used in this work

The SILAM model versions, setup and input data used in the papers are shown in Table 3.1.

In **Paper I** the aerosol concentration and composition over Europe was computed by four regional chemistry-transport models - CMAQ, EMEP, LOTOS-EUROS and SILAM. The setup of the models is shown in Table 3.2.

The anthropogenic emissions originated from the TNO-TRANSPHORM inventory (*Denier van der Gon et al.*, 2014). The wild-land fire emissions were provided by the Integrated System for wild-land fires IS4FIRES (*Sofiev et al.*, 2009; *Soares*

Table 3.1: SILAM setups used in the studies

Model setup	**Paper I**	**Paper II**	**Paper III**	**Paper IV**	**Paper V**
Model version	SILAM v5.3	SILAM v5.3	SILAM v4.5	SILAM v5.2	SILAM v5.1
Direction	Forward	Forward	Forward, Adjoint	Forward	Adjoint
Species	All PM components	Wild-fire emitted $PM_{2.5}$	SOx, PM	Ragweed pollen	Grass pollen
Transport	Eulerian	Eulerian	Eulerian, Lagrangian	Eulerian	Eulerian
Area	Europe	Europe	15°E-42°E; 58°N–72°N	Europe	Europe
Period	2005	2005, 2008	2003, 2006	2005-2011	2009-2011
Resolution	0.3° x 0.2°	0.3° x 0.2°	0.1°	0.2°	0.3° x 0.2°
Vertical	8 layers up to ∼8km	8 layers up to ∼8km	11 layers up to ∼9km	8 layers up to ∼7km	8 layers up to ∼6km
Timestep	15 min	15 min	6 min	15 min	15 min
Meteorology	ECMWF	ECMWF	ECMWF, HIRLAM	ECMWF	ECMWF
Emission	TNO-TRANSPHORM (*Denier van der Gon et al.*, 2014)	IS4FIRES	EMEP	**Paper IV**	Observed pollen potency

et al., 2015). Desert dust was included only through the lateral boundary conditions; no wind-blown dust was emitted inside the modelling domain.The collected model output consisted of hourly concentrations of each PM component, separately for fine ($PM_{2.5}$) and coarse ($PM_{2.5-10}$) fractions: SO_4^{2-}, NO_3^- and NH_4^+, EC, OC, SOA, sea salt, mineral dust, wild-land fire originated particulate matter, unspeciated other primary PM, and additionally also total $PM_{2.5}$ and PM_{10} fields. Not all components were available from all models – OC was provided as a separate species only by EMEP and CMAQ models; forest fire smoke was left out of the total PM output of EMEP and LOTOS-EUROS but was provided as a separate field, while in CMAQ the fine fraction of fire emitted PM was included in primary OA and the coarse fraction in unspeciated coarse primary PM.

Models also computed the concentration of benzo[a]pyrene (BaP), which was assumed to be an inert fine aerosol not participating in any chemical transformations.

Paper II used the SILAM simulations from **Paper I** to assess the health effects of wildfire smoke in Europe. An extra SILAM run was made for wild-land fire smoke 2008 with identical model setup.

In this thesis the footprint analysis has been applied for both supporting the analysis of observations (**Paper V**) and for refining the emission estimates (**Paper III**). In **Paper III**, the footprints of model-measurement discrepancies at the Värriö station lead to the discovery of an error in the emission data of the met-

Table 3.2: Model setup for the TRANSPHORM multi-model intercomparison. Table 1 from Paper I)

Model	CMAQ v4.7.1	EMEP MSC-W rv. 4.4	LOTOS-EUROS v1.8	SILAM v5.3
Horizontal resolution	18 km	0.2° x 0.2°	0.3° x 0.2°	0.3° x 0.2°
Vertical resolution	34 layers up to ∼20 km	20 layers up to 100 hPa	3 layers up to 3.5 km	8 layers up to ∼8km
Lowest layer	∼20m	∼90m; 3m concentrations derived from the lowest layer values	the mixing layer; 25m surface layer for tracking surface concentrations	20m
Meteo driver	WRF v3.2.1	ECMWF	ECMWF	ECMWF
Chemistry scheme	CB05	EMEP EmChem09 *Simpson et al.* (2012)	TNO CBM-IV	Acid-Basic *Sofiev* (2000)
Aerosol scheme	aero5	MARS and VBS *Bergström et al.* (2012)	ISORROPIA2	Extended DMAT *Sofiev* (2000)
Temporal emission profiles	*Builtjes et al.* (2003)	*Simpson et al.* (2012)	*Builtjes et al.* (2003)	EuroDelta
Vertical emission profiles	SMOKE plume rise based on *Briggs* (1971), wildfire emission homogeneously up to 1km	*Simpson et al.* (2012), wildfire emission homogeneously up to 1km	EURODELTA *Cuvelier et al.* (2007), wildfire emission homogeneously up to 1km	*Bieser et al.* (2011), *Sofiev et al.* (2012) for fire emissions
Wildfire emission	IS4FIRES v1 *Sofiev et al.* (2009)	IS4FIRES v1 *Sofiev et al.* (2009)	IS4FIRES v1 *Sofiev et al.* (2009)	IS4FIRES v2 *Soares et al.* (2015)
Sea salt emission	*Spicer et al.* (1998)	*Tsyro et al.* (2011)	*Mårtensson et al.* (2003); *Monahan et al.* (1986)	*Sofiev et al.* (2011)
Reference	*Foley et al.* (2010)	*Simpson et al.* (2012)	*Schaap et al.* (2008), *Wichink Kruit et al.* (2012)	*Sofiev et al.* (2015b)

allurgy plants on Kola Peninsula. After correcting the emission data, combined adjoint and forward modelling was applied to analyse whether further refinements were possible.

In **Paper V** the allergen observation footprints were used for mapping the source areas of pollen with different potency. The model evaluated the transport for 60 hours backward in time for each daily observation at each site. The observed pollen potency was mapped to the origin of pollen via the footprints, which were cut off at 99%, and only the areas where the grass was predicted to be flowering at

the time were kept, so that the remaining footprint would cover the sources that contributed 99% of the observation. A weighted mean of the attributed potency values was computed over the season, the weights taking into account the predicted flowering intensity in the gridcell and the footprint value. The computations resulted in potency maps, which show the mean potency of pollen released from the area during a specific year.

Chapter 4

Results and discussion

4.1 Modelling the particulate matter in Europe

4.1.1 The ability of chemical transport models to simulate the mass concentration and composition of PM

The currently available chemical transport models commonly under-predict the PM mass concentrations, however the previous multi-model studies have not thoroughly investigated how this underprediction is reflected in the PM chemical composition. The study presented in **Paper I** was conducted to quantify the model deficiencies in terms of the aerosol chemical constituents, source categories, seasonal variations, and geographical distribution. The aerosol predictions of four widely used chemical transport models (CMAQ, EMEP, LOTOS-EUROS and SILAM) were compared to the chemically-speciated PM observations by the EMEP monitoring network.

When the calculated dry PM mass was compared with the measurements, all models systematically underestimated PM_{10} and $PM_{2.5}$ by 10-60%, depending on the model and the season of the year, as shown in Figure 4.1. The PM components for which the modelling and monitoring experience is longer, such as nitrates, sulphates and ammonia were reproduced fairly well by all the models, whereas there were major underestimations for carbonaceous and mineral aerosols (Table 4.1).

SO_4 and NH_4 were mostly slightly underestimated by the models, while the NO_3 concentrations were mostly somewhat overestimated. While the models reproduced the summertime drop in the concentrations of NH_4 and NO_3, they tended to overestimate the autumn concentrations, and while the observations show the highest concentrations in spring for all three secondary inorganic aerosol (SIA) species, this was not reproduced by the models. SILAM did not reproduce the seasonal variations well - it overestimated NO_3 in winter and SO_4 in autumn and underestimated NH_4 in summer.

The sea-salt concentrations were mostly overestimated by the models. SILAM failed to reproduce the seasonal variations in the sea salt concentration, the other models reproduced it more successfully.

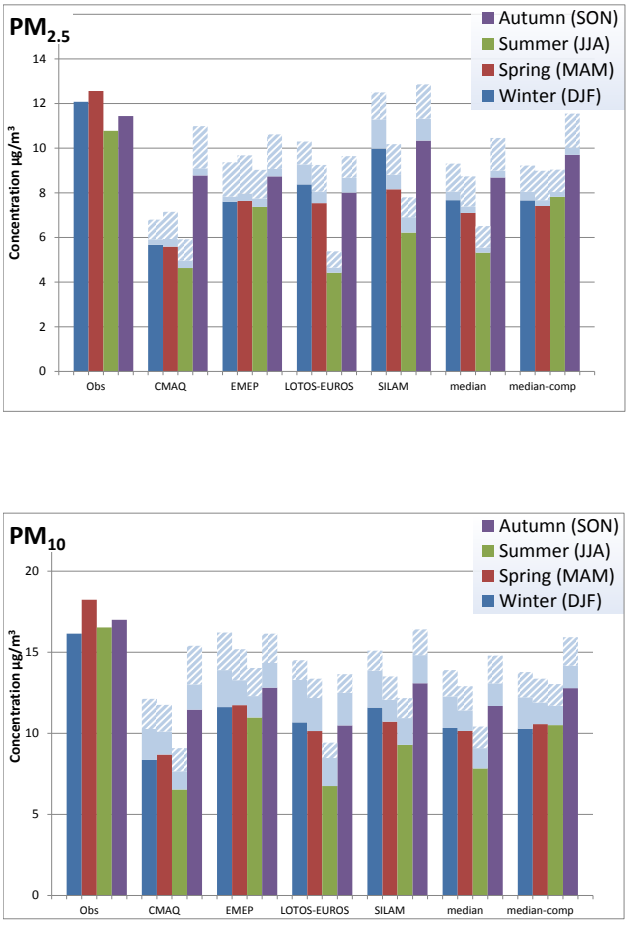

Figure 4.1: Observed and predicted seasonal concentrations of $PM_{2.5}$ (upper panel) and PM_{10} (lower panel), mean over the EMEP stations [μg PM m^{-3}]. The light blue part shows the aerosol-bound water amount at the filter weighting conditions (50% relative humidity, 20° C), estimated with ISORROPIA2 based on the modelled aerosol composition. The solid light blue shows the water content in stable case (the lower curve of the hysteresis loop) and the striped part in metastable case (the upper branch of the hysteresis loop), when the crystallization has not occurred to aerosol coming from more humid conditions. Figure 3 of **Paper I**.

Only SILAM and EMEP modelled the transport of desert dust from the boundaries (mainly Sahara) as a separate tracer. A 10% Ca content was assumed for it, and in addition, a 3.5% Ca content was attributed to the mineral part of primary

Table 4.1: Annual statistics for the PM components: ScaledBias - bias divided with the mean observed value, tCor - temporal correlation of the daily values, Fac2 – the fraction of daily values within factor of two from the observed ones. The shading emphasizes the range of the values – bias: blue - underestimation, orange - overestimation; correlation and factor-2 agreement: red - low, green - high. Table 7 of **Paper I**.

Species	Model	Scaled bias	tCor	Fac2	Species	Model	Scaled bias	tCor	Fac2
NH_4	*CMAQ*	-0.08	0.55	0.49	**NO_3**	*CMAQ*	-0.12	0.35	0.47
Ave obs:	*EMEP*	-0.08	0.58	0.51	*Ave obs:*	*EMEP*	0.13	0.46	0.45
0.86 µg N/m ^{3}	*LOTOS-EUROS*	-0.06	0.56	0.47	*0.52 µg N/m ^{3}*	*LOTOS-EUROS*	0.06	0.44	0.42
	SILAM	-0.16	0.55	0.37		*SILAM*	0.06	0.44	0.39
	median	-0.13	0.61	0.5		*median*	0.00	0.49	0.49
NH_3+NH_4	*CMAQ*	0.00	0.38	0.44	**NO_3+HNO_3**	*CMAQ*	0.14	0.49	0.67
Ave obs:	*EMEP*	-0.06	0.45	0.59	*Ave obs:*	*EMEP*	0.24	0.49	0.56
1.54 µg N/m ^{3}	*LOTOS-EUROS*	0.12	0.39	0.59	*0.58 µg N/m ^{3}*	*LOTOS-EUROS*	0.12	0.47	0.6
	SILAM	0.10	0.44	0.54		*SILAM*	0.02	0.48	0.49
	median	0.01	0.47	0.6		*median*	0.10	0.54	0.65
NH_3	*CMAQ*	0.04	0.18	0.25	**HNO_3**	*CMAQ*	0.21	0.34	0.43
Ave obs:	*EMEP*	-0.07	0.30	0.36	*Ave obs:*	*EMEP*	-0.11	0.38	0.39
0.75 µg N/m ^{3}	*LOTOS-EUROS*	0.19	0.22	0.38	*0.19 µg N/m ^{3}*	*LOTOS-EUROS*	0.00	0.38	0.40
	SILAM	0.32	0.30	0.40		*SILAM*	-0.53	0.32	0.32
	median	0.05	0.31	0.39		*median*	-0.16	0.41	0.44
SO_4	*CMAQ*	-0.10	0.59	0.73	**SO_2**	*CMAQ*	0.25	0.53	0.49
Ave obs:	*EMEP*	-0.18	0.58	0.57	*Ave obs:*	*EMEP*	0.23	0.47	0.48
0.77 µg S /m ^{3}	*LOTOS-EUROS*	-0.38	0.56	0.45	*0.79 µg S/m ^{3}*	*LOTOS-EUROS*	0.05	0.49	0.54
	SILAM	-0.04	0.51	0.52		*SILAM*	-0.13	0.48	0.5
	median	-0.23	0.63	0.63		*median*	0.04	0.55	0.54
Sea salt	*CMAQ*	0.40	0.48	0.46	**Mineral dust**	*EMEP*	-0.75	0.29	0.29
Ave obs:	*EMEP*	0.38	0.54	0.49	*Ave obs:*	*SILAM*	-0.58	0.31	0.33
0.78 µg Na/m ^{3}	*LOTOS-EUROS*	-0.03	0.38	0.49	*0.12 µg Ca/m ^{3}*	*median*	-0.67	0.32	0.31
	SILAM	0.08	0.44	0.48					
	median	0.13	0.55	0.58					
EC in $PM_{2.5}$	CMAQ	-0.61	0.51	0.35	**EC in PM_{10}**	CMAQ	-0.69	0.42	0.32
Ave obs:	EMEP	-0.56	0.53	0.4	*Ave obs:*	EMEP	-0.66	0.46	0.35
1.08 µg C/m^3	LOTOS-EUROS	-0.34	0.51	0.44	1.32 µg C/m^3	LOTOS-EUROS	-0.48	0.39	0.44
	SILAM	-0.17	0.61	0.4		SILAM	-0.35	0.45	0.38
	median	-0.45	0.6	0.38		median	-0.58	0.49	0.37
OC in $PM_{2.5}$	CMAQ	-0.80	0.52	0.26	**OC in PM_{10}**	CMAQ	-0.85	0.36	0.18
Ave obs:	EMEP	-0.25	0.54	0.6	*Ave obs:*	EMEP	-0.37	0.46	0.52
3.61 µg C/m^3	median	-0.52	0.54	0.61	4.78 µg C/m^3	median	-0.61	0.46	0.48

anthropogenic emissions. The modelled contributions from these sources are about equal, except for winter when the models predict almost no dust from Sahara. The

non-sea-salt calcium (nss-Ca) concentrations are substantially underestimated by the models for the whole year. The EMEP model underestimated the nss-Ca by 75% and SILAM by 58%. Considering that the models omitted the wind-blown dust emissions inside the European modelling domain, this underestimation is not surprising. The seasonal patterns of the models differ from the observations, where the autumn concentrations are close to the winter levels and noticeably lower than for summer. The models rather suggest similar dust levels for most of the year, except for winter when the predicted concentrations are lower.

The model evaluation for the carbonaceous compounds suffers from the limited amount of available observational data and for OC also model data was provided only by two of the models (SILAM and LOTOS-EUROS did not compute SOA formation). Only four EMEP stations reported the EC and OC concentrations in 2005. However, based on the data from these stations and additional data from EMEP 2002-2003 campaign, it could be concluded that the concentrations of the carbonaceous components are severely underestimated. The models reproduce the seasonal variations observed in EC concentrations, but they completely miss the observed OC winter maximum. The large underestimation in winter could be caused by missing emissions of domestic heating (*Denier van der Gon et al.*, 2015), but also the SOA formation from anthropogenic aromatics could be underestimated. A rather large portion of semi-volatile organics is believed to be missing in current anthropogenic emission inventories of $PM_{2.5}$ and NMVOCs (*Denier van der Gon et al.*, 2015; *Donahue et al.*, 2006; *Ots et al.*, 2016b; *Robinson et al.*, 2007). Cooking emissions have been pointed out as another missing source of organic aerosols (*Fountoukis et al.*, 2015; *Young et al.*, 2015; *Ots et al.*, 2016a). The large model-to-model differences for EC were somewhat surprising, as the emission data had been unified and no chemical transformations affect the EC concentrations in the atmosphere. A possible explanation is the considerably lower dry deposition of fine aerosols in SILAM (*Kouznetsov and Sofiev*, 2012). Different treatment of EC hygroscopicity and ageing, affecting the efficiency of its wet scavenging, could also contribute to differences in the model results.

The benzo(a)pyrene concentrations were overestimated by all models, which was also unexpected, as the models underestimate the concentrations of black carbon and the sources of these two pollutants significantly overlap. One possible reason for this can be a simplified approach taken by the models to simulate this species: BaP was assumed to be an inert fine aerosol not participating in chemical transformations and not partitioning to gas-phase. In more complex models the heterogeneous oxidation by ozone has been reported to efficiently reduce the BaP concentrations (*Friedman and Selin*, 2012; *Matthias et al.*, 2009). It is also probable that some part of the over-estimation, especially in winter time when the oxidation is slower, may be attributed to the emissions.

The individual PM components were reproduced with about the same or lower quality as the total PM. Not all individual PM components were equally underestimated. The secondary inorganic species were reproduced without much bias and sea salt was usually overestimated. Large underestimations for carbonaceous and mineral aerosols were supported by the few available observations. In some cases the overestimations of some components could bring the models very close or even

over the observed PM levels, while still underestimating other components.

The ensemble median showed better correlation with the observations than the individual models. However, the bias demonstrated by all models propagated also into the median results. This effect can be reduced by computing the median for each of the PM components separately with subsequent summation to the total-PM concentration. This procedure reduces the effect of the components that have been omitted by some of the models within the ensemble.

4.1.2 The most important components contributing to the PM deficit

The study highlighted the importance of the contribution of commonly omitted aerosol components, such as SOA, mineral dust and wildfire smoke. Neglecting the desert dust contribution to the PM budget substantially worsened the correlation of model predictions with PM observations in summer, which indicates that accounting for the inflow of Saharan dust is important in PM simulations, especially for southern Europe - for central and northern parts, agricultural and road dust are more important on an annual basis. The impact of wild-land fires was also significant in summer of 2005 in the western and southern parts of the domain. Including SOA in the modelled PM also substantially reduced the model bias in summer. Providing that all major PM components are included, the particle-bound water in gravimetric PM observations can explain a major fraction of the remaining bias. Based on the modelled aerosol composition, the average water content at laboratory conditions was estimated roughly between 5 and 20% for $PM_{2.5}$ and between 10 and 25% for PM_{10}, depending on whether the aerosol was assumed to be in stable or metastable state, the latter corresponding to situation when the aerosol has been exposed to more humid conditions and crystallization has not occurred. Adding this contribution to the modelled PM reduced the model bias 25–70 % (Table 4.2, Figure 4.1), but also reduced both spatial and temporal correlations with the observations.

The estimated aerosol water content on the filters is in the range of the previous estimates of *Tsyro* (2005), who estimated 20-35% water content for the aerosol observed in EMEP stations and *Sillanpää et al.* (2006), who estimated up to 20% water content for the urban aerosol observations.

Several uncertainties exist estimating the PM water content, that could explain the reduction of the correlation coefficients. Firstly, the water content depends on the outdoor humidity at the measurement location as well as the filter transportation and storage conditions, so it cannot be determined, whether the aerosol is in stable or metastable branch of the hysteresis cycle. Secondly, ISORROPIA2 computes the water content based on the inorganic part of aerosol – SIA, sea salt, calcium; it does not take into account the water related to the hydrophilic part of the organic aerosol, which could also influence the water uptake of the inorganic species (*Jing et al.*, 2015). Thirdly, the aerosols were assumed fully internally mixed, which lowers the deliquescence humidity compared to external mixtures and might lead to overestimation of water uptake. Overestimating hydrophilic compounds, such as sea salt can also lead to overestimation of the water content

Table 4.2: Annual statistics for the $PM_{2.5}$ and PM_{10}, dry mass, aerosol bound water added assuming stable state (lower curve of the hysteresis loop) and metastable state (higher curve of the hysteresis loop). ScaledBias - bias divided with the mean observed value, tCor - temporal correlation of the daily values, Fac2 – the fraction of daily values within factor of two from the observed ones. The shading emphasizes the range of the values – bias: blue - underestimation, orange - overestimation; correlation and factor-2 agreement: red - low, green - high. Table 6 of **Paper I**.

		Dry			*50% relative humidity, 20° C, stable*			*50% relative humidity, 20° C, metastable*		
Species	**Model**	**Scaled bias**	**tCor**	**Fac2**	**Scaled bias**	**tCor**	**Fac2**	**Scaled bias**	**tCor**	**Fac2**
$PM_{2.5}$ *Ave obs: 11.78 μg/m^3*	*CMAQ*	-0.47	0.50	0.47	-0.44	0.50	0.50	-0.34	0.49	0.58
	EMEP	-0.33	0.62	0.69	-0.30	0.62	0.71	-0.17	0.62	0.77
	LOTOS-EUROS	-0.40	0.46	0.51	-0.34	0.43	0.54	-0.26	0.45	0.58
	SILAM	-0.26	0.59	0.58	-0.18	0.57	0.61	-0.08	0.57	0.64
	median	-0.38	0.63	0.61	-0.35	0.63	0.63	-0.26	0.63	0.70
	medianComp	-0.30	0.60	0.62	-0.28	0.60	0.64	-0.17	0.60	0.71
PM_{10} *Ave obs: 17.09 μg/m^3*	*CMAQ*	-0.49	0.46	0.49	-0.40	0.42	0.53	-0.29	0.41	0.59
	EMEP	-0.31	0.57	0.69	-0.21	0.51	0.70	-0.09	0.51	0.72
	LOTOS-EUROS	-0.44	0.40	0.53	-0.32	0.29	0.57	-0.25	0.32	0.61
	SILAM	-0.34	0.54	0.54	-0.24	0.50	0.58	-0.16	0.51	0.60
	median	-0.41	0.59	0.59	-0.33	0.53	0.63	-0.23	0.54	0.68
	medianComp	-0.35	0.57	0.63	-0.26	0.53	0.66	-0.17	0.54	0.70

in PM. Also, in addition to the particle-bound water, the filters themselves can accumulate humidity and influence the measurement results (*Brown et al.*, 2006).

4.1.3 Comparison with other similar studies

Other model inter-comparison studies have been published, evaluating the models ability to reproduce the observed concentrations of either PM or some of its components. Some of those studies use similar set of observations (daily measurements of the EMEP network) and some of the participating models are the same as in **Paper I**, but different model versions, set-ups and input data are used. Although these studies concentrate on different time periods, some conclusions about how well **Paper I** describes the general skill of PM modelling can still be made by comparing the results with those studies.

Solazzo et al. (2012a) compared the AQMEII (Air Quality Model Evaluation International Initiative) ensemble with the PM observations from EMEP and AirBase databases for 2006 and *Im et al.* (2014) compared the AQMEII2 ensemble with similar set of measurements for 2010. *Solazzo et al.* (2012a) report underestimation of PM_{10} in Europe ranging from 20 to 65%, with two outlying models overestimating by about 5%. Temporal correlations of the daily average PM_{10} values ranged from 0.2 to 0.7, lowest correlations shown by the overestimating models, indicating significant modelling errors in those models. The AQMEII 2 results are

very similar – *Im et al.* (2014) report all models underestimating PM_{10} in the rural stations by 20 to 66 %. Correlation coefficients for the daily values ranged from 0.2 to 0.86. $PM_{2.5}$ was overestimated by one model by 20%, with almost zero correlation, all other models underestimated by up to 60%, with correlations ranging from 0.1 to 0.84. These results are very similar to the **Paper I** evaluation, where comparing the dry PM with daily EMEP observations resulted in annual mean biases between 25 and 50% and correlations from 0.4 to 0.62.

A few multi-model assessments have previously been published for the SIA components. *Hass et al.* (2003) presented the evaluation of six EUROTRAC models simulating SIA and its precursors in Europe in the summer half-year of 1995. The models were compared with the daily EMEP observations, making the results comparable with those of **Paper I**. Compared with **Paper I** the EUROTRAC models showed much wider range of biases, but most of the models still overestimated NO_3 and underestimated SO_4, same as found in **Paper I**. The best EUROTRAC models (*Hass et al.*, 2003) outperformed those of **Paper I** for both temporal correlation and factor-two agreement fractions.

The EURODELTA seven-model ensemble was compared with the EMEP obsevations for the year 2001 by *Vautard et al.* (2009), who also found the sulphate aerosols generally underestimated while nitrate was overestimated and ammonium modelled in a more balanced way. The correlation coefficients for SIA for individual models of EURODELTA ensemble ranged from 0.4 to 0.7, being slightly higher than those shown in **Paper I**.

A comprehensive model evaluation was presented by (*Bessagnet et al.*, 2014) for the seven model ensemble of EURODELTA III (ED-3), comparing both gases and particulates, although against only one month of observations. The models were evaluated against EMEP intensive observation campaign and routine measurements from 25th of February to 26th of March 2009.

Similarily to **Paper I**, most of the ED-3 models somewhat overestimated sea salt and heavily underestimated dust concentrations (the modelled dust concentrations were compared with calcium observations multiplied by eight), although most models in ED-3 emitted wind-blown dust inside the modelling domain . The correlation coefficients for dust were very low, which was also the case in **Paper I**. The underestimation of the carbonaceous aerosols was also confirmed in the ED-3 study. All models underestimated the measured total organic matter concentrations in both fine and coarse fractions by 50 to 80%. The models underestimated EC in $PM_{2.5}$ up to $\sim$50%, while the coarse EC was overestimated. In **Paper I** the coarse EC and OC could not be reliably evaluated, as the emission of coarse anthropogenic PM was not split to components and was modelled as a single substance.

SIA components were underestimated by some ED-3 models and overestimated by others, only ammonia was more often overestimated. Correlation coefficients for nitrates and ammonium were around 0.6-0.75, and somewhat lower for sulphates (0.3-0.55). This differs from **Paper I**, where the spring-time concentrations of SIA components were mostly slightly underestimated, and sulphates showed better correlation with observations than nitrates. The springtime emission of NH_3 strongly depends on meteorological conditions and crop fertilizing practices, whereas in the

models fixed annual cycle of emission intensity is used. On some years this fixed cycle can reflect the real meteorology worse than on others and thus lead to poorer correlations between the models and the observations for the related compounds, making the modelling different years not directly comparable.

For $PM_{2.5}$ and PM_{10}, an extended comparison with wider selection of EMEP observations (four month-long intensive campaigns from 2006 to 2009) is presented by *Bessagnet et al.* (2016). Most of the ED-3 models underestimated PM_{10} for all campaigns by ∼20-30%, while $PM_{2.5}$ was reproduced with smaller negative bias an sometimes even slightly overestimated by some models. The smaller bias than shown in **Paper I** can be explained by the fact that of the aerosol components mostly omitted in **Paper I**, most models in ED-3 had emissions for wind-blown dust and computed SOA formation. Correlations with the daily observations were similar to those in **Paper I**- around 0.6 for $PM_{2.5}$ and around 0.5 for PM_{10}, with the exception of the summer campaign 2006, when several models showed correlations above 0.7 for PM_{10}. Similarly wide range of spatial correlations as was shown in **Paper I** (0.06-0.86) for different models and seasons was also shown by *Bessagnet et al.* (2016) for the different campaigns (0.05-0.8).

All in all, the multi-model comparison studies published since 2003 have shown very similar results for the models ability to reproduce the observed concentrations of PM components in the background stations in Europe. Carbonaceous and crustal components have been pointed out as the major contributors to the underestimation of particulate matter.

4.2 Estimating the health effects of the PM from wild-land fires

In **Paper I**, using the IS4FIRES v1 emissions in EMEP and LOTOS-EUROS models resulted in degradation of the model scores for $PM_{2.5}$ and PM_{10}, the correlations for EC and OC also reduced when fire contribution was added. In SILAM a newer version of the emission data was used (IS4FIRES v2, *Soares et al.* (2015), together with the dynamic emission vertical profiles of *Sofiev et al.* (2012), while in other models the IS4FIRES v1 emission data was spread evenly to the first 1000 m. Mainly due to the vertical profiles that release most of the smoke high aloft, the ground level concentrations of fire PM were substantially lower in SILAM and the fire PM did not negatively affect the model performance. This result encouraged us to use the SILAM predictions of wild-fire smoke in **Paper II** to assess annual mortality attributable to short-term exposures to vegetation-fire originated $PM_{2.5}$ in different regions in Europe. An extra model simulation was made to estimate the wildfire emitted PM in 2008 with the same model setup as in **Paper I**.

The large-scale distributions of the vegetation-fire emitted $PM_{2.5}$ in 2005 and 2008 were similar: the fires were intensive mainly in northern Portugal and Spain, southern Italy, the Balkans, the Black Sea area, the Kaliningrad area and other parts of western Russia (Figure 4.2). The main difference between the two years was in the relative strength of the fires in the southern and eastern regions, which is partly explained by the differences in temperature and precipitation in 2005 and

2008 – year 2005 was hot and dry in the Iberian Peninsula, leading to a large number of vegetation fires, whereas the cold and wet conditions in 2008 led to relatively few fires. In contrast, in the Balkan region and southern Italy year 2008 was hotter and dryer than average, resulting in more severe fires compared to 2005.

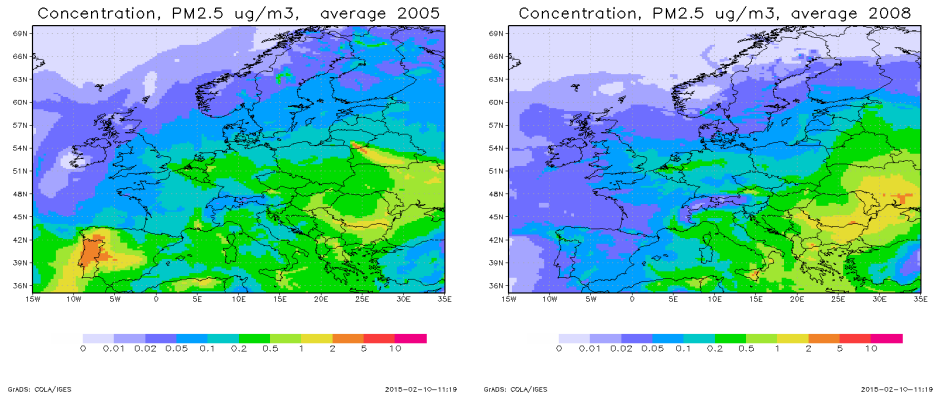

Figure 4.2: Modelled wildfire originated $PM_{2.5}$ concentration [$\mu g\ m^{-3}$], average over 2005 (left) and 2008 (right).

Mortality impacts were assessed for 27 European countries based on the modelled daily wild-fire induced $PM_{2.5}$ concentrations, population data, and the exposure-response function of *Zanobetti and Schwartz* (2009) for short-term $PM_{2.5}$ exposure, combined with the country-level data for background mortality risk. In the EU 27 countries, more than thousand premature deaths were attributable to the vegetation-fire originated $PM_{2.5}$ annually. The highest impacts were found in southern and eastern Europe. However, all countries were affected by fire $PM_{2.5}$, and the lower concentrations in western and northern Europe also contributed significantly (30%) to the overall attributable mortality. The estimates suggest that the majority (70-80%) of the premature deaths attributable to fire-originated $PM_{2.5}$ in 2005 and 2008 were caused by low to moderate increases in daily concentrations (<15 $\mu g/m^3$), particularly in the western and northern regions where $PM_{2.5}$ increases of <2 $\mu g/m^3$ and<15 $\mu g/m^3$ were estimated to have caused 60-80% and > 98% of premature deaths, respectively. The assessment suggests that air pollution due to $PM_{2.5}$ released from vegetation fires is a relevant risk factor for public health in Europe, and the risk is expected to increase in the future as climate change proceeds.

4.3 Improvement of emission data

Analysis of the different emission inventories, observational campaigns and regular air quality monitoring in Northern Lapland, land-use, and sectoral emission

split allowed detecting problems with the total emission of Kola Peninsula and its distribution in the EMEP and other existing inventories. In the EMEP data the emission of the Nikel metallurgy plant was found to be misallocated to the Murmansk city region. A refined emission for Kola Peninsula was suggested, keeping the totals at the level of the pre-2006 reported EMEP estimates and redistributing the industrial part of the emission from the city of Murmansk to the location of the Nikel metallurgy plant.

The consideration was based on individual SNAP sectors. Assuming that the emission of SNAP sector S1 (large combustion in energy and transformation industry) is dominated by the Nikel plant, the S1 emissions in Murmansk area were moved to the Nikel plant location, leaving in the original grid cells only a small fraction, corresponding to the S1 level in the neighbouring cells. Similar logic was applied to other sectors and species that contribute to the infrastructure of a large factory (S2, S3), summing up to roughly 115 kilotons of SO_2 per year.

Using forward and adjoint simulations of the SILAM system, the suggested emission correction was verified against two years of regular SO_2 monitoring data in Northern Lapland and the PM measurement campaign at Värriö in 2003. The long-term model-measurement comparison showed sharp reduction of the model underestimation (up to slight over-estimation in the nearest vicinity to the plant) and noticeable improvement of the temporal correlation. However, even with the updated emissions the model still underestimated the SO_2 and SO_4 concentrations and SO_4 wet deposition in majority of the stations, and the adjoint modelling indicated that the underestimation originated from the Nikel area (Figure 4.3), suggesting that the revised emission amount could still be underestimated.

Table 4.3 shows the currently available SO_x emission estimates from various sources. The most accurate SO_x emission data for Kola Peninsula is available from the Arctic Monitoring and Assessment Programme (AMAP). *AMAP* (2006) reports 150 kt SO_2 emitted from the Zapolyarnyi an Nikel metallurgy plants in 2000. Very similar amounts are reported for 2009 by *Hongisto* (2014) – 136 kt/year SO_2 emissions in Nikel and Zapoljarnyi – referring to a presentation no longer available on the website of the operator of the plants. These numbers are 25-30% higher than the assessment of **Paper III**, explaining at least partly the underestimation still remaining in the modelling results after the emission correction was applied.

For PM, the four model runs based on the two different transport modules of SILAM and meteorological input from ECMWF and HIRLAM showed widely varying results in reproducing the observed peak in Värriö. The model also missed majority of the $PM_{2.5}$ most of the time, partly due to the underestimations also in other emitted species and source sectors, but also due to missing PM components, as the simulations included only anthropogenic primary PM and the SIA precursors. Thus, nothing conclusive could be said about the accuracy of the emission correction based on the PM observations in Värriö. Due to the uncertainties introduced by the sparse observational network, and inaccuracies in the emission vertical distribution and SO_x wet deposition, the further refinement of the Kola Peninsula emissions assessment methods was recommended using activity data.

As reported by *Hongisto* (2014) and *Eckhardt et al.* (2015), errors in the emissions of the industrial sources of Kola Peninsula are still common in the emission

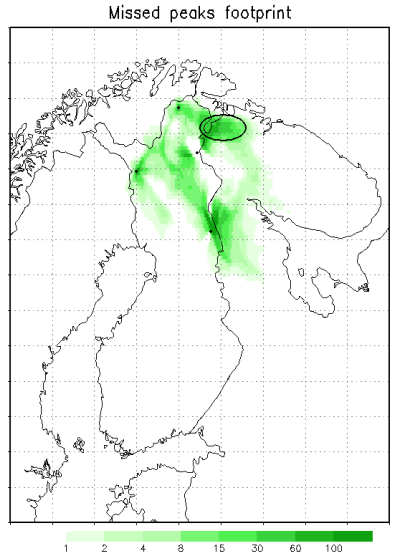

Figure 4.3: Footprint of the major model-measurement differences (mdl-obs) of SO_2 concentration at monitoring sites (black dots), when the model was run with the revised emission estimates. The higher footprint values indicate the areas where the revised SO_2 emission is likely to be underestimated. The black circle surrounds the Nikel area. Presence of hot-spots around individual stations is an artefact originating from the low density of the observational network. Figure 10 of **Paper III**.

Table 4.3: SO_x emission from large sources on Kola Peninsula (Unit: kilotons of SO_2 per grid cell per year).

Data source	Year	Nikel	Murmansk	Monchegorsk	Kola total
EMEP <2006	2003	4.9	157.0	130.0	291.9
EMEP 2009	2003	0.2	10.9	11.5	22.7
EMEP 2016	2003	7.0	1.9	10.8	19.7
EMEP 2016	2000	6.8	3.0	10.6	20.5
EMEP 2016	2009	6.2	1.4	9.3	16.9
Paper III	2003	114.5	47.3	130.0	291.9
AMAP	2000	150		45	
Hongisto (2014)	2009	136			
TNO-MACC III	2000	∼30			∼80
TNO-MACC III	2010	∼50			∼110
EDGAR v4.3	2010	6.6			38
ECLIPSE v4a	2005				∼33

databases. In 2015 the emissions in EMEP database have again been recomputed. Table 4.3 shows that the currently available SO_x emissions have a more realistic pattern - higher than average SO_x emissions are visible in the Nikel plant location

for all years. However, emission amounts are still about 10 times too low (Table 4.3). In the TNO-MACC-III inventory (*Kuenen et al.*, 2014), the SO_2 emissions in the period of 2000 to 2010 rise from ∼30 to ∼50 ktons in the Nikel location and form ∼80 to ∼110 kt in the whole Kola Peninsula. In EDGAR v4.3 (*Crippa et al.*, 2016) 6.6 kt of SO_2 are emitted in Nikel location in 2010 and 38 kt in the whole Peninsula. *Eckhardt et al.* (2015) reports that also in ECLIPSE version 4a inventory only about 33 kt of SO_2 are emitted in the Kola area for the year 2005.

4.4 Pollen modelling

4.4.1 Modelling the emission and dispersion of ragweed pollen

In order to provide timely warnings for the allergy sufferers, a model was developed for forecasting ragweed pollen concentrations in the air. An emission module was developed, incorporating the phenological development of the plant and pollen release from the inflorescences. The pollen transport by wind, mixing by turbulence, deposition via sedimentation and scavenging by precipitation was evaluated by the standard SILAM routines. The annual total ragweed pollen emission and the predicted average seasonal pollen index (SPI, the sum of daily average pollen counts over the pollen season) are shown on Figure 4.4.

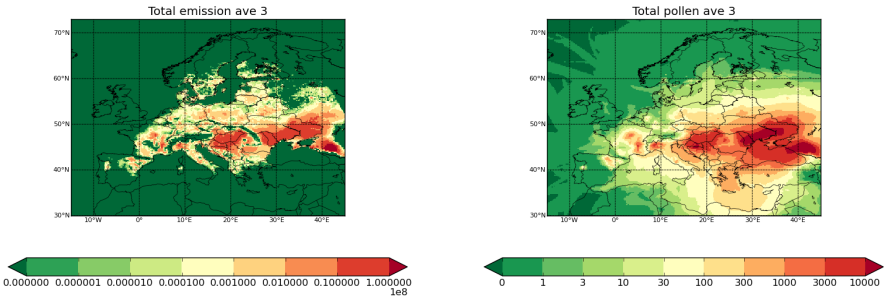

Figure 4.4: Average annual ragweed pollen emission [pollen m^{-2} $year^{-1}$] (left) and seasonal pollen index (sum of daily mean concentrations [pollen m^{-3}]) (right).

The evaluation of the new model against multi-annual ragweed pollen observations from the EAN network demonstrated that the model reproduces well the main ragweed pollen season in the areas with major plant presence, such as the Pannonian Plain, the Lyon area in France, the Milan region in Italy, as well as areas in Ukraine and southern Russia. The predicted start of the season was mostly within 3 days of the observed for the majority of stations in these areas. The temporal correlation between modelled and observed concentrations exceeded 0.6 for the bulk of the stations. The hit rate exceeded 0.8 in the main source regions for

the exceedances of allergy-relevant concentration thresholds (5 and 20 pollen/m^3) and the false alarm ratio stayed below 10% (Figure 4.5).

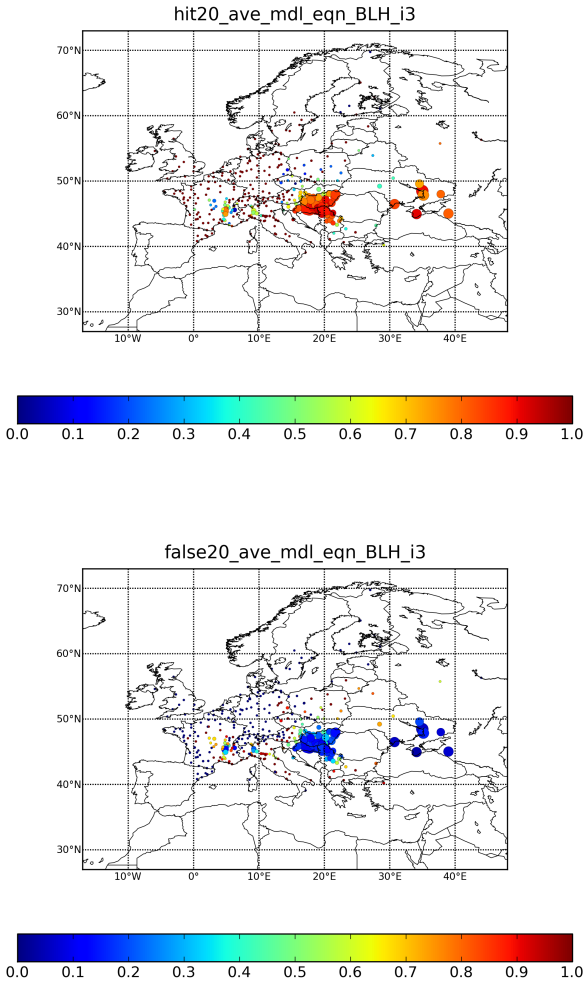

Figure 4.5: Ragweed pollen forecast hit rate (upper panel) and false alarm ratio (lower panel) for exceeding 20 pollen threshold. Middle panels of Figure 9 of **Paper IV**.

The application of the new model outlined the areas of significant probability of exceedances of allergy-relevant thresholds, showing that the strong south-north gradient of ragweed presence and prevailing west-to-east transport direction, together with natural barriers for pollen dispersion, such as mountains, reduced ragweed pollen levels in northern and western-most parts of Europe. However, it

also highlighted the important role of long-range atmospheric transport in forming the high-concentration patterns - during the long-range transport episodes, high concentrations can be recorded virtually anywhere in Europe, summing up to several days of harmful pollen levels per year even in regions remote from the heavily invaded areas. As such, our modelling illustrates the potential for a relatively localised invasive species to produce impacts on human health at a continental scale.

Leiblein-Wild et al. (2015) developed a more complex model for predicting the timing of the ragweed phenological phases and emitted pollen amount. The model of *Leiblein-Wild et al.* (2015) uses 95% of maximum day length as the trigger for the start of flowering and thus predicts earlier start of the season in north than in south, while in SILAM the season is supposed to start when the days get shorter than 14.5 hours, leading to earlier flowering in south. A north-south gradient is visible on Figure 4.6 for the model bias in predicting the season start for the Pannonian Plain, the most infested area with a well covering observational network, with the model being late in the northern stations and a few days early in the southernmost ones. This indicates that the phenological model of *Leiblein-Wild et al.* (2015) might be more realistic.

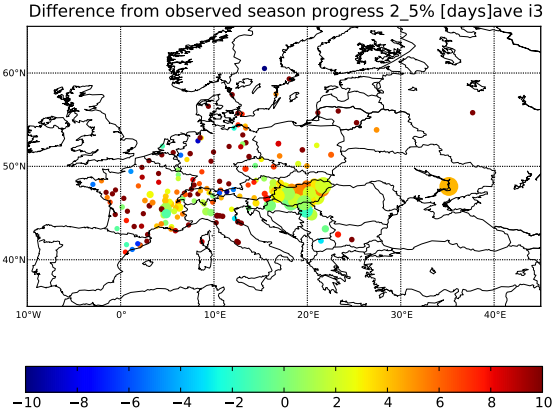

Figure 4.6: Model-measurement difference for the start of the flowering season [days], calculated from predicted and observed 2.5% of seasonal pollen count. Left panel of Figure 4 of **Paper IV**.

In SILAM, the current ragweed occupancy map of *Chapman et al.* (2016) was calibrated with observations to obtain the map of annual pollen emission. The ragweed emissions from Ukraine and southern Russia needed to be increased significantly in order to reproduce the pollen observations in these areas. This resulted in that area becoming the most infested in Europe. The ragweed habitat and pollen emission maps produced by *Leiblein-Wild et al.* (2015) and *Storkey et al.* (2014) do not shown a high infestation in that area. *Cunze et al.* (2013) did not predict high suitability there with the model based on the European occupancy observations,

while the model based on the native North American data predicted the area highly suitable for ragweed.

The climatic suitability and invasion models that produced the ragweed maps used in SILAM are described in *Chapman et al.* (2014, 2016); *Bullock et al.* (2012). Extention of ragweed habitat towards north is predicted for the future climate, while decrease is foreseen for the southern populations due to droughts. The SILAM computations of ragweed pollen in future climate are shown in *Bullock et al.* (2012). A similar study was recently published by *Hamaoui-Laguel et al.* (2015), using the ragweed distribution of *Storkey et al.* (2014). They also predict the habitat extending northwards, though do not agree with its decline in south. *Cunze et al.* (2013) predicts further spread northwards and potential extinction in parts of the current habitat for some climate scenarioes. *Leiblein-Wild et al.* (2015) found large parts of Europe climatically suitable for ragweed growth and reproduction, and reported a higher invasion potential than currently achieved in western Europe and along parts of the northern edge of its distribution, expecting the invasion to continue in these directions.

The comparison of the quality of the SILAM predictions for the six pollen species adapted from *Prank et al.* (2016) is shown in Table 4.4. The best modelled species is ragweed, with the spatial correlation of the seasonal pollen index (SPI, sum of daily mean pollen concentrations over the pollen season) of 0.91 and the modelled season start within 3 days from the observed in 54% of the cases. Season start is also well reproduced for birch, the only species where the flowering model has been calibrated based on phenological observations, not pollen counts.

The worst scores are shown for grass pollen, where the correlation is almost zero and a large bias exists for the SPI. This stresses the need of calibration of the habitat map with the pollen observations, to take into account the plants pollen productivity in different climatic zones, and also to correct the errors in the underlying land-use data. Following the comparison presented here (from *Prank et al.* (2016)), the grass pollen model in SILAM has been recently recalibrated and the forecasts for the last pollen season (summer 2016) were already made with improved model.

For all species, the end of the season is reproduced by the model with lower quality than the beginning, with noticeable biases for several species. However, the accuracy of the forecasts of season end is much less relevant for the allergy patients than the accuracy of predicting the start of the season, which is required for starting their medications in time.

One of the reasons for the low quality in predicting the seasons end is that in the model the season is assumed to have a single peak. However, in the observations seasons with multiple peaks are relatively common. This can be caused by several species with somewhat different flowering times producing indistinguishable pollens. Another reason for errors in the flowering time can be temperature accumulation in unresolved mountain terrains and seaside, where the large model grid cell covers microenvironments with noticeably different conditions.

Table 4.4: Model performance for different pollen species. Norm. bias – bias normalized with the observed average concentration, Correlation – spatial correlation of observed and modelled SPI values over the stations, Fac2 - fraction of cases (stations, years) when modelled SPI is within factor of 2 from the observation, Season start/mid/end – day when 5%, 50% or 95% of the total SPI is reached, <nDays – Fraction of cases when SILAM is within n days from the observed season start, midpoint or end. The shading emphasizes the range of the values – bias: blue - underestimation, red - overestimation; other scores: white - low, green - high.

	Birch	Grass	Olive	Ragweed	Mugwort	Alder
Seasonal pollen index						
Correlation	0.52	0.02	0.66	0.91	0.72	0.65
Norm bias	-0.19	1.53	-0.06	0.08	0.02	-0.09
Fac2	0.68	0.45	0.31	0.68	0.75	0.72
Start 5% day						
Bias (days)	0.31	4.60	-9.51	3.02	4.49	-0.47
<3Day	0.50	0.25	0.28	0.54	0.39	0.35
<7Day	0.73	0.46	0.46	0.81	0.69	0.55
Mid 50% day						
Bias (days)	3.49	9.99	-11.07	0.79	2.37	-2.65
<3Day	0.50	0.17	0.34	0.63	0.27	0.33
<7Day	0.73	0.33	0.54	0.88	0.48	0.54
End 95% day						
Bias (days)	2.25	-2.00	-18.89	-1.53	-5.69	-13.11
<3Day	0.38	0.20	0.19	0.45	0.27	0.23
<7Day	0.61	0.40	0.36	0.77	0.51	0.40

4.4.2 Studying the variability of pollen allergenicity

HIALINE project was launched with the purpose to study the natural variability in release of the major allergen groups from the pollen of birch, grass and olive trees across Europe (Bet v 1, Phl p 5 and Ole e 1, respectively). Co-located daily pollen and allergen measurements were made in 8 stations over Europe during the pollen seasons of 2009 to 2011. The average daily pollen potency was computed by dividing the allergen concentration in air with the observed pollen amount. The findings for birch and olive pollen have been published by *Buters et al.* (2012) and *Galan et al.* (2013), and **Paper V** analyses the variations in grass pollen potency. Large variations in the potency were found for all three species (Figure 4.7). Grass pollen showed a larger natural variability in allergen release than birch or olive pollen, ranging from less than 1 to 9 pg of Phl p 5 per pollen (5th to 95th percentile). About 10% of the captured grass pollen released no group 5 allergen at all. This fraction was noticeably larger than the fraction of cases with low pollen potency (up to 0.5 pg of allergen per pollen), which is not the case for birch and olive. Large variability in grass pollen potency is expected, as the pollens from different grass species, although identical for pollen observations, are known to include different

amounts of different allergens. In **Paper V** the observed variability was shown to be larger than would arise from the experimental errors, proving that the observations are sensitive enough to capture the day-to-day changes.

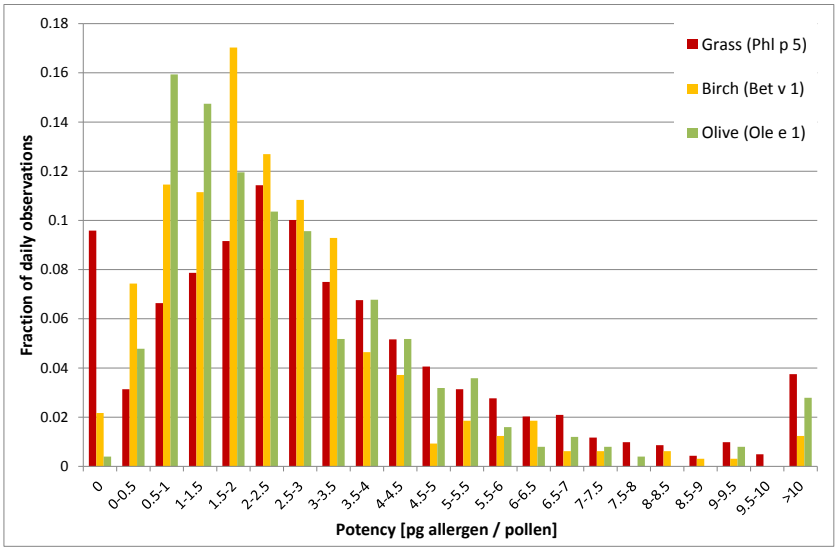

Figure 4.7: Histograms of daily average pollen potency (allergen release per pollen [pg pollen^{-1}]) for birch, grass and olive pollen, observed during the HIALINE project.

It can be expected that around every station several grass species contribute to the grass pollen count, and the main contributors can differ between the regions. Changing wind direction can bring pollen to the station from areas where different grass species are abundant. In addition to different habitat preferences, the grass species also flower at somewhat different times, so the grass pollen potency can also change during the season. Year-to-year variability could arise from different species being successful on different years.

In addition, allergen-releasing particles were found in $PM_{2.5-10}$, although this size-fraction of aerosol should not contain any intact pollens, as the grass pollens are mostly 20 - 40 μm in diameter. The Phl p 5 amount in $PM_{2.5-10}$ correlated with ambient humidity.

Some differences in potency related to the geographical origin of the pollen had been noticed before for birch and olive (*Buters et al.*, 2012; *Galan et al.*, 2013). The origin of the observed pollen (the observation footprint) was computed by adjoint modelling with SILAM for every daily observation. In order to study the relation of the grass pollen potency to the source area, the footprints were scaled with the

observed pollen potency and combined into annual average potency maps. The average potency map over the three years (2009-2011) can be seen on the upper panel of Figure 4.8. While some regions, such as France, consistently appeared to have higher potency of the emitted pollen (reaching above 5 pg of Phl p 5 per pollen) and the Easter Europe showed lower potency in all years (going below 2 pg of Phl p 5 per pollen), in most regions the potency appeared to vary from year to year. Due to these large variations no clear geographic pattern of pollen potency was detected.

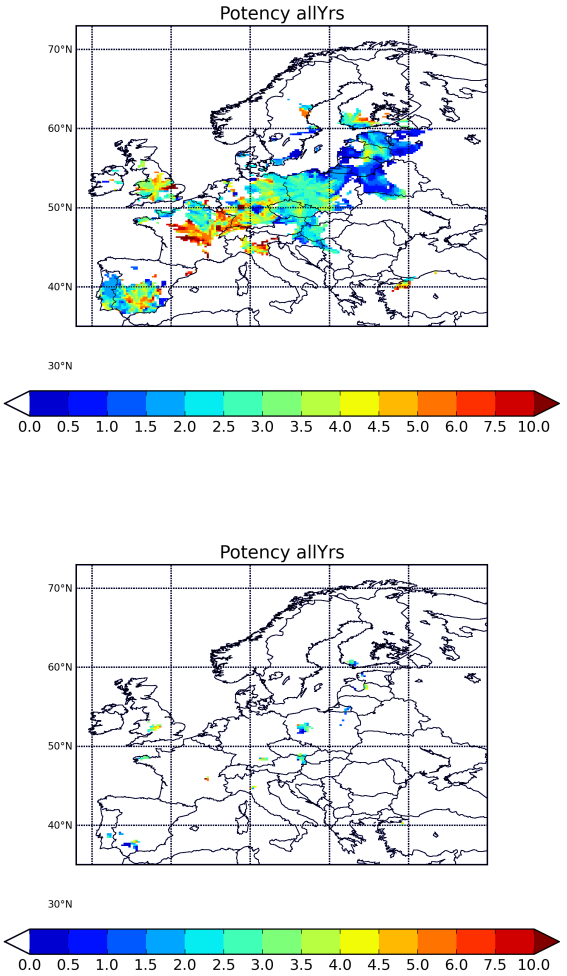

Figure 4.8: Grass pollen potency maps [pg pollen^{-1}] for 99% footprint (upper panel) and 67% footprint (lower panel), mean 2009-2011

Due to the large size of the grass pollen (mostly 30-40 μm) their lifetime in atmosphere is short. In **Paper V**, in order to avoid mapping potency values to the areas with very low probability to contribute noticeably to the measurement, the footprints that were used for making the potency maps were cut so that they covered the area where 99% of the observed pollen originated. The lower panel of Figure 4.8 is based on footprints that represent the source area of two thirds of the observed pollen, showing that majority of the pollen reaching the stations originates only from a small number of grid cells in the vicinity to the station, so the potency of the pollen emitted further from the stations is increasingly uncertain.

Chapter 5

Conclusions and future outlook

Atmospheric composition has strong influence on human health, ecosystems and also Earth's climate. Thus, reliable estimates of emissions and distributions of pollutants are necessary for assessing the future climate and air-quality related health effects. Chemistry-transport models are valuable tools for understanding the processes influencing the atmospheric composition. The thesis presents a collection of developments and applications of the chemistry-transport model SILAM.

SILAM's ability to reproduce the observed aerosol composition was evaluated and compared with three other commonly used CTM-s in Europe in **Paper I**. When the calculated dry PM mass was compared with the measurements, all models systematically underestimated PM_{10} and $PM_{2.5}$ by 10-60%, depending on the model and the season of the year. For majority of the PM chemical components, the relative underestimation was smaller than that, exceptions being the carbonaceous particles and mineral dust – species that suffer from relatively small amount of available observational data.

The study highlighted the importance of the contribution of commonly omitted aerosol components, such as the secondary organic aerosols (SOA), mineral dust and wildfire smoke and stressed the necessity for high-quality emissions from these sources. Neglecting the desert dust contribution to the PM budget substantially worsened the correlation of model predictions with PM observations in summer, which indicates that accounting for the inflow of Saharan dust is important in PM simulations, especially for southern Europe. For the central and northern parts of Europe, agricultural and road dust are more important on an annual basis. Including SOA in the modelled PM also substantially reduced the model bias in summer. The impact of wild-land fires was also significant in summer of 2005 in the western and southern parts of the domain. The need for high quality wildfire emission data was pointed out. Providing that all major PM components are included, the particle-bound water in gravimetric PM observations can explain a major fraction of the remaining bias. The average water content at laboratory conditions was estimated between 5 and 20% for $PM_{2.5}$ and between 10 and 25%

for PM_{10}.

SILAM produced the annual mean level of the secondary inorganic aerosol (SIA) with similar quality as the other models, but did not reproduce well the seasonal variations. In the future the parametrizations of SIA formation in SILAM, including the heterogeneous SO_2 oxidation, gas-particle equilibrium of NH_4NO_3 and the seasonality of NH_3 emissions, will have to be revised. Indications were also found that the temperature dependence of the sea salt emissions might be overestimated in SILAM. Regarding the omitted species, the chemistry-transformation schemes in SILAM have been extended to include the formation of SOA and the work on dust emissions is ongoing.

SILAM had the smallest bias in $PM_{2.5}$ among the models, largely owing to the high quality wild-fire emission data from IS4FIRES v2 – in EMEP and LOTOS-EUROS models that used IS4FIRES v1 data, inclusion of this component decreased the modelling quality of PM significantly and thus it was omitted from their total PM fields. The good quality of SILAM wild-fire smoke predictions encouraged us to use the predictions in an health impact assessment study. The predictions were used to assess the annual mortality attributable to short-term exposures to vegetation-fire originated $PM_{2.5}$ in different regions in Europe. $PM_{2.5}$ emitted from vegetation fires was found to be a relevant risk factor for public health in Europe, more than 1000 premature deaths per year were attributed to vegetation-fire released $PM_{2.5}$.

Air quality predictions depend critically on emission data quality. An error was found in the EMEP anthropogenic emission inventory regarding the SO_x and PM emissions of metallurgy plants on the Kola Peninsula and a correction was suggested and evaluated using SILAM in bot forward and adjoint modes. However, this problem is still evident in several currently available emission inventories.

Allergenic pollen is arguably the type of aerosol with most widely recognised effect on health. SILAM's ability to predict allergenic pollen was extended to include common ragweed (*Ambrosia Artemisiifolia* L) - an invasive weed spreading in Southern Europe, with extremely allergenic pollen capable of inducing rhinoconjuctivitis and asthma in the sensitive individuals even in very low concentrations. The model could reproduce the ragweed pollen levels with similar or better accuracy than it had for the previously modelled species and operational forecasts have been made for ragweed pollen for the last three years.

The future plans in SILAM pollen modelling include further extensions of the species list, also considering allergenic fungal spores. Regarding the species already in the model, it will be relevant to start modelling the inter-annual variations in the plant pollen production - currently the same plant is assumed to produce exactly the same amount of pollen every year and this is known to lead to large errors in the forecast. Another possible development foreseen in the future is to start accounting for the variable potency of pollen grains – as shown by *Buters et al.* (2012); *Galan et al.* (2013) and **Paper V** the amount of allergen in birch, grass and olive pollen can vary noticeably from day to day. Thus, although the pollen counts are an excellent proxy for exposure, more can be learned from the actual monitoring and modelling of allergens in ambient air.

In **Paper V** the variations of allergenicity in grass pollen were studied and mapped to the source areas by adjoint runs with SILAM. Due to the high variabil-

ity of observed pollen potency, the results were not conclusive. For grass pollen this is not surprising, as visually indistinguishable pollens are released by many grass species, and the pollen allergen content varies between the different species. Similar kind of mapping could provide more interesting results for the other species measured at the same campaign – indications of pollen potency dependence on the area of its origin was found for both birch *Buters et al.* (2012) and olive *Galan et al.* (2013).

Bibliography

Aiken, A. C., P. F. DeCarlo, J. H. Kroll, D. R. Worsnop, J. A. Huffman, K. S. Docherty, I. M. Ulbrich, C. Mohr, J. R. Kimmel, D. Sueper, Y. Sun, Q. Zhang, A. Trimborn, M. Northway, P. J. Ziemann, M. R. Canagaratna, T. B. Onasch, M. R. Alfarra, A. S. H. Prevot, J. Dommen, J. Duplissy, A. Metzger, U. Baltensperger, and J. L. Jimenez, O/C and OM/OC ratios of primary, secondary, and ambient organic aerosols with high-resolution time-of-flight aerosol mass spectrometry, *Environmental Science & Technology*, *42*(12), 4478–4485, doi:doi:10.1021/es703009q, 2008.

Akagi, S. K., R. J. Yokelson, C. Wiedinmyer, M. J. Alvarado, J. S. Reid, T. Karl, J. D. Crounse, and P. Wennberg, Emission factors for open and domestic biomass burning for use in atmospheric models, *Atmospheric Chemistry and Physics Discussions*, *11*, 4039–4072, doi:10.5194/acp-11-4039-2011, 2011.

AMAP, Arctic Pollution 2006: Acidification and Arctic Haze, *Tech. rep.*, Arctic Monitoring and Assessment Programme (AMAP), Oslo, Norway, 2006.

Andersen, T. B., A model to predict the beginning of the pollen season, *Grana*, *30*(1), 269–275, doi:10.1080/00173139109427810, 1991.

Andreae, M. O., and P. Merlet, Emission of trace gases and aerosols from biomass burning, *Global biogeochemical cycles*, *15*(4), 955–966, 2001.

Atkinson, R. W., I. C. Mills, H. A. Walton, and H. R. Anderson, Fine particle components and health—a systematic review and meta-analysis of epidemiological time series studies of daily mortality and hospital admissions, *Journal of Exposure Science and Environmental Epidemiology*, *25*, 208–214, doi:10.1038/jes.2014.63, 2015.

Avila, A., M. Alarcón, and I. Queralt, The chemical composition of dust transported in red rains—its contribution to the biogeochemical cycle of a holm oak forest in Catalonia (Spain), *Atmospheric Environment*, *32*(2), 179–191, doi:10.1016/S1352-2310(97)00286-0, 1998.

Barney, J. N., and A. Ditommaso, The biology of Canadian weeds . 118 . Artemisia vulgaris L ., *Canadian Journal of Plant Science*, *83*, 205–215, doi:10.4141/P01-098, 2003.

Belis, C., F. Karagulian, B. Larsen, and P. Hopke, Critical review and meta-analysis of ambient particulate matter source apportionment using receptor models in Europe, *Atmospheric Environment*, *69*, 94–108, doi:10.1016/j.atmosenv.2012.11.009, 2013.

Bergström, R., H. a. C. Denier van der Gon, a. S. H. Prévôt, K. E. Yttri, and D. Simpson, Modelling of organic aerosols over Europe (2002-2007) using a volatility basis set (VBS) framework: application of different assumptions regarding the formation of secondary organic aerosol, *Atmospheric Chemistry and Physics*, *12*(18), 8499–8527, doi:10.5194/acp-12-8499-2012, 2012.

Bessagnet, B., A. Colette, F. Meleux, L. Rouïl, A. Ung, O. Favez, K. Cuvelier, P. Thunis, S. Tsyro, R. Stern, A. Manders, R. Kranenburg, A. Aulinger, J. Bieser, M. Mircea, G. Briganti, A. Cappelletti, G. Calori, S. Finardi, C. Silibello, G. Ciarelli, S. Aksoyoglu, A. Prévot, M. T. Pay, M. Baldasano, M. García Vivanco, J. L. Garrido, I. Palomino, F. Martín, G. Pirovano, P. Roberts, L. Gonzalez, L. White, L. Menut, J.-C. Dupont, C. Carnevale, and A. Pederzoli, The EURODELTA III exercise – Model evaluation with observations issued from the 2009 EMEP intensive period and standard measurements in Feb / Mar 2009, *Tech. rep.*, Technical EMEP report 1/2014, TFMM & MSC-W Technical Report, CLRTAP, Geneva, 2014.

Bessagnet, B., G. Pirovano, M. Mircea, C. Cuvelier, A. Aulinger, G. Calori, G. Ciarelli, A. Manders, R. Stern, S. Tsyro, M. García Vivanco, P. Thunis, M.-T. Pay, A. Colette, F. Couvidat, F. Meleux, L. Rouïl, A. Ung, S. Aksoyoglu, J. M. Baldasano, J. Bieser, G. Briganti, A. Cappelletti, M. D'Isodoro, S. Finardi, R. Kranenburg, C. Silibello, C. Carnevale, W. Aas, J.-C. Dupont, H. Fagerli, L. Gonzalez, L. Menut, A. S. H. Prévôt, P. Roberts, and L. White, Presentation of the EURODELTA III inter-comparison exercise - Evaluation of the chemistry transport models performance on criteria pollutants and joint analysis with meteorology, *Atmospheric Chemistry and Physics Discussions*, (January), 1–61, doi:10.5194/acp-2015-736, 2016.

Bieser, J., A. Aulinger, V. Matthias, M. Quante, and H. A. C. D. V. D. Gon, Vertical emission profiles for Europe based on plume rise calculations, *Environmental Pollution*, *159*(10), 2935–2946, doi:10.1016/j.envpol.2011.04.030, 2011.

Briggs, G. A., Some Recent Analyses of Plume Rise Observation, in *Proceedings of the Second International Clean Air Congress*, edited by H. M. Englun and W. T. Beery, pp. 1029–1032, Academic Press, New York, 1971.

Brown, A., R. Yardley, P. Quincey, and D. Butterfield, Studies of the effect of humidity and other factors on some different filter materials used for gravimetric measurements of ambient particulate matter, *Atmospheric Environment*, *40*(25), 4670–4678, doi:10.1016/j.atmosenv.2006.04.028, 2006.

Brus, D. J., G. M. Hengeveld, D. J. J. Walvoort, P. W. Goedhart, A. H. Heidema, G. J. Nabuurs, and K. Gunia, Statistical mapping of tree species over Europe, *European Journal of Forest Research*, *131*(1), 145–157, doi:10.1007/s10342-011-0513-5, 2012.

Builtjes, P. J. H., M. van Loon, M. Schaap, S. Teeuwisse, A. J. H. Visschedijk, J. P. Bloos, A. Visschedijnk, and J. P. Bloos, Project on the Modelling and Verification of Ozone Reduction Strategies: Contribution of TNO-MEP, *Tech. rep.*, TNO-Report, MEP-R2003/166, Apeldoorn, The Netherlands, 2003.

Bullock, J. M., S. M. White, C. Prudhomme, C. Tansey, R. Perea, and D. a. P. Hooftman, Modelling spread of British wind-dispersed plants under future wind speeds in a changing climate, *Journal of Ecology*, *100*(1), 104–115, doi:10.1111/j.1365-2745.2011.01910.x, 2012.

Buters, J., M. Prank, M. Sofiev, G. Pusch, R. Albertini, I. Annesi-Maesano, C. Antunes, H. Behrendt, U. Berger, R. Brandao, S. Celenk, C. Galan, L. Grewling, B. Jackowiak, R. Kennedy, A. Rantio-Lehtimäki, G. Reese, I. Sauliene, M. Smith, M. Thibaudon, B. Weber, and L. Cecchi, Variation of the group 5 grass pollen allergen content of airborne pollen in relation to geographic location and time in season, *Journal of Allergy and Clinical Immunology*, *136*(1), 87–95, doi:10.1016/j.jaci.2015.01.049, 2015.

Buters, J. T., M. Thibaudon, M. Smith, R. Kennedy, A. Rantio-Lehtimäki, R. Albertini, G. Reese, B. Weber, C. Galan, R. Brandao, C. M. Antunes, S. Jäger, U. Berger, S. Celenk, Ł. Grewling, B. Jackowiak, I. Sauliene, I. Weichenmeier, G. Pusch, H. Sarioglu, M. Ueffing, H. Behrendt, M. Prank, M. Sofiev, and L. Cecchi, Release of Bet v 1 from birch pollen from 5 European countries. Results from the HIALINE study, *Atmospheric Environment*, *55*, 496–505, doi:10.1016/j.atmosenv.2012.01.054, 2012.

Cassee, F. R., M.-E. Heroux, M. E. Gerlofs-Nijland, and F. J. Kelly, Particulate matter beyond mass: recent health evidence on the role of fractions, chemical constituents and sources of emission, *Inhalation Toxicology*, *25*(14), 802–812, doi:10.3109/08958378.2013.850127, 2013.

Champeaux, J. L., V. Masson, and F. Chauvin, ECOCLIMAP: a global database of land surface parameters at I km resolution, *Meteorological Applications*, *12*(1), 29–32, doi:10.1017/S1350482705001519, 2005.

Chapman, D. S., T. Haynes, S. Beal, F. Essl, and J. M. Bullock, Phenology predicts the native and invasive range limits of common ragweed., *Global change biology*, *20*(1), 192–202, doi:10.1111/gcb.12380, 2014.

Chapman, D. S., L. Makra, R. Albertini, M. Bonini, A. Páldy, V. Rodinkova, B. Sikoparija, E. Weryszko-Chmielewska, and J. M. Bullock, Modelling the introduction and spread of non-native species: International trade and climate change drive ragweed invasion, *Global Change Biology*, doi:10.1111/gcb.13220, 2016.

Colette, A., C. Andersson, A. Baklanov, B. Bessagnet, J. Brandt, J. H. Christensen, R. Doherty, M. Engardt, C. Geels, C. Giannakopoulos, G. B. Hedegaard, E. Katragkou, J. Langner, H. Lei, A. Manders, D. Melas, F. Meleux, L. Rouïl, M. Sofiev, J. Soares, D. S. Stevenson, M. Tombrou-Tzella, K. V. Varotsos, and P. Young, Is the ozone climate penalty robust in Europe?, *Environmental Research Letters*, *10*(8), 084,015, doi:10.1088/1748-9326/10/8/084015, 2015.

Crippa, M., G. Janssens-Maenhout, F. Dentener, D. Guizzardi, K. Sindelarova, M. Muntean, R. Van Dingenen, and C. Granier, Forty years of improvements in European air quality: regional policy-industry interactions with global impacts, *Atmospheric Chemistry and Physics*, *16*(6), 3825–3841, doi:10.5194/acp-16-3825-2016, 2016.

Cunze, S., M. C. Leiblein, and O. Tackenberg, Range Expansion of Ambrosia artemisiifolia in Europe Is Promoted by Climate Change, *ISRN Ecology*, *2013*, 1–9, doi:10.1155/2013/610126, 2013.

Cuvelier, C., P. Thunis, R. Vautard, M. Amann, B. Bessagnet, M. Bedogni, R. Berkowicz, J. Brandt, F. Brocheton, P. Builtjes, A. Coppalle, B. Denby, G. Douros, A. Graf, O. Hellmuth, C. Honor'e, A. Hodzic, J. Jonson, A. Kerschbaumer, F. de Leeuw, E. Minguzzi, P. Wind, and A. Zuber, CityDelta: a model intercomparison study to explore the impact of emission reductions in European cities in 2010, *Atmos. Environ*, *41*, 189–2007, 2007.

Dahl, Å., C. Galán, L. Hajkova, A. Pauling, B. Sikoparija, M. Smith, and D. Vokou, The Onset, Course and Intensity of the Pollen Season, in *Allergenic Pollen*, edited by M. Sofiev and K.-C. Bergmann, chap. 3, pp. 29–70, Springer Netherlands, Dordrecht, doi:10.1007/978-94-007-4881-1_3, 2013.

Dai, L., A. Zanobetti, P. Koutrakis, and J. D. Schwartz, Associations of Fine Particulate Matter Species with Mortality in the United states: A Multicity Time-Series Analysis, *Environmental Health Perspectives*, *122*(8), 837–842, doi:10.1289/ehp.1307568, 2014.

de Weger, L. A., K. C. Bergmann, A. Rantio-Lehtimäki, Å. Dahl, J. Buters, C. Déchamp, J. Belmonte, M. Thibaudon, L. Cecchi, J.-P. Besancenot, C. Galán, and Y. Waisel, Impact of Pollen, in *Allergenic Pollen: A Review of the Production, Release, Distribution and Health Impacts*, edited by M. Sofiev and K.-C. Bergmann, chap. 6, pp. 161–215, Springer Netherlands, Dordrecht, doi:10.1007/978-94-007-4881-1_6, 2013.

Deen, W., L. A. Hunt, and C. J. Swanton, Photothermal time describes common ragweed (Ambrosia artemisiifolia L .) phenological development and growth, *Weed Science*, *46*, 561–568, 1998.

Denier van der Gon, H. A. C., A. Visschedijk, J. Kuenen, U. K. R van Gijlswijk, C. Schieberle, J. Theloke, and R. Friedrich, European Emission baseline (final dataset) for 2005 incl. specific transport emission grids and projection to 2020/30 dataset, Deliverable Report D1.3.5; EU FP7 TRANSPHORM (ENV.2009.1.2.2.1 Transport related air pollution and health impacts); revised vers, *Tech. rep.*, Deliverable Report D1.3.5, EU FP7 TRANSPHORM (ENV.2009.1.2.2.1 Transport related air pollution and health impacts), revised version, January 2014, 2014.

Denier van der Gon, H. a. C., R. Bergström, C. Fountoukis, C. Johansson, S. N. Pandis, D. Simpson, and a. J. H. Visschedijk, Particulate emissions from residential wood combustion in Europe – revised estimates and an evaluation, *Atmospheric Chemistry and Physics*, *15*(11), 6503–6519, doi:10.5194/acp-15-6503-2015, 2015.

Dennis, R., T. Fox, M. Fuentes, A. Gilliland, S. Hanna, C. Hogrefe, J. Irwin, S. T. Rao, R. Scheffe, K. Schere, D. Steyn, and A. Venkatram, A framework for evaluating regional-scale numerical photochemical modeling systems, *Environmental Fluid Mechanics*, *10*(4), 471–489, doi:10.1007/s10652-009-9163-2, 2010.

Dentener, F., T. Keating, and H. Akimoto, Hemispheric transport of air pollution 2010. PART A: OZONE AND PARTICULATE MATTER, *Tech. rep.*, Task Force on Hemispheric Transport of Air Pollution, Geneva, 2010.

Donahue, N. M., a. L. Robinson, C. O. Stanier, and S. N. Pandis, Coupled partitioning, dilution, and chemical aging of semivolatile organics, *Environmental Science and Technology*, *40*(8), 2635–2643, doi:10.1021/es052297c, 2006.

Eckhardt, S., B. Quennehen, D. J. L. Olivié, T. K. Berntsen, R. Cherian, J. H. Christensen, W. Collins, S. Crepinsek, N. Daskalakis, M. Flanner, A. Herber, C. Heyes, Ø. Hodnebrog, L. Huang, M. Kanakidou, Z. Klimont, J. Langner, K. S. Law, A. Massling, S. Myriokefalitakis, I. E. Nielsen, J. K. Nøjgaard, J. Quaas, P. K. Quinn, J.-C. Raut, S. T. Rumbold, M. Schulz, R. B. Skeie, H. Skov, M. T. Lund, T. Uttal, K. von Salzen, R. Mahmood, and A. Stohl, Current model capabilities for simulating black carbon and sulfate concentrations in the Arctic atmosphere: a multi-model evaluation using a comprehensive measurement data set, *Atmospheric Chemistry and Physics*, *15*, 9413–9433, doi:10.5194/acpd-15-10425-2015, 2015.

EMEP, C., Manual for Sampling and Chemical Analysis, *Tech. rep.*, 2001.

Estrella, N., A. Menzel, U. Krämer, and H. Behrendt, Integration of flowering dates in phenology and pollen counts in aerobiology: Analysis of their spatial and temporal coherence in Germany (1992-1999), *International Journal of Biometeorology*, *51*(1), 49–59, doi:10.1007/s00484-006-0038-7, 2006.

Flesch, T. K., J. D. Wilson, and E. Yee, Backward-Time Lagrangian Stochastic Dispersion Models and Their Application to Estimate Gaseous Emissions, doi:10.1175/1520-0450(1995)034<1320:BTLSDM>2.0.CO;2, 1995.

Foley, K. M., S. J. Roselle, K. W. Appel, P. V. Bhave, J. E. Pleim, T. L. Otte, R. Mathur, G. Sarwar, J. O. Young, R. C. Gilliam, and Others, Incremental testing of the Community Multiscale Air Quality (CMAQ) modeling system version 4.7, *Geoscientific Model Development*, *3*(1), 205–226, 2010.

Formenti, P., L. Schütz, Y. Balkanski, K. Desboeufs, M. Ebert, K. Kandler, A. Petzold, D. Scheuvens, S. Weinbruch, and D. Zhang, Recent progress in understanding physical and chemical properties of African and Asian mineral dust, *Atmospheric Chemistry and Physics*, *11*(16), 8231–8256, doi:10.5194/acp-11-8231-2011, 2011.

Fountoukis, C., and A. Nenes, ISORROPIA II : a computationally efficient thermodynamic equilibrium model for K+-Ca2+-Mg2+-NH4+-Na+-SO42–NO3–Cl–H2O aerosols, *Atmospheric Chemistry and Physics*, *7*(17), 4639–4659, 2007.

Fountoukis, C., A. G. Megaritis, K. Skyllakou, P. E. Charalampidis, H. A. C. Denier van der Gon, M. Crippa, A. S. H. Prévôt, F. Freutel, A. Wiedensohler, C. Pilinis, and S. N. Pandis, Simulating the formation of carbonaceous aerosol in a European Megacity (Paris) during the MEGAPOLI summer and winter campaigns, *Atmospheric Chemistry and Physics Discussions*, *15*(18), 25,547–25,582, doi:10.5194/acpd-15-25547-2015, 2015.

Friedman, C. L., and N. E. Selin, Long-range atmospheric transport of polycyclic aromatic hydrocarbons: a global 3-D model analysis including evaluation of Arctic sources., *Environmental science & technology*, *46*(17), 9501–10, doi:10.1021/es301904d, 2012.

Fritz, S., L. See, I. McCallum, C. Schill, M. Obersteiner, M. van der Velde, H. Boettcher, P. Havlík, and F. Achard, Highlighting continued uncertainty in global land cover maps for the user community, *Environmental Research Letters*, *6*(4), 044,005, doi:10.1088/1748-9326/6/4/044005, 2011.

Fumanal, B., B. Chauvel, and F. Bretagnolle, Estimation of pollen and seed production of common ragweed in France, *Annals of Agriculture and Environmental Medicine*, *14*, 233–236, 2007.

Galan, C., H. Garcia-Mozo, L. Vazquez, L. Ruiz, D. L. Guardia, C. Diaz, and M. M. Trigo, Heat requirement for the onset of the Olea europaea L. pollen season in several sites in Andalusia and the effect of the expected future climate change, *International Journal of Biometeorology*, *49*(3), 184–188, doi:10.1007/s00484-004-0223-5, 2005.

Galan, C., C. Antunes, R. Brandao, C. Torres, H. Garcia-Mozo, E. Caeiro, R. Ferro, M. Prank, M. Sofiev, R. Albertini, U. Berger, L. Cecchi, S. Celenk, L. Grewling, B. Jackowiak, S. Jäger, R. Kennedy, A. Rantio-Lehtimäki, G. Reese, I. Sauliene, M. Smith,

M. Thibaudon, B. Weber, I. Weichenmeier, G. Pusch, J. T. Buters, and T. H. working Group, Airborne olive pollen counts are not representative of exposure to the major olive allergen Ole e 1, *Allergy*, doi:doi:10.1111/all.12144, 2013.

Gery, M., G. Whitten, J. Killus, and M. Dodge, A photochemical kinetics mechanism for urban and regional scale computer modeling, *Journal of Geophysical Research*, *94*(12), 925–12, 1989.

Grewling, B. Sikoparija, C. A. Skjoth, P. Radisic, D. Apatini, D. Magyar, A. Paldy, R. Yankova, J. Sommer, I. Kasprzyk, D. Myszkowska, A. Uruska, M. Zimny, M. Puc, S. Jäger, and M. Smith, Variation in Artemisia pollen seasons in Central and Eastern Europe, *Agricultural and Forest Meteorology*, *160*, 48–59, doi:10.1016/j.agrformet.2012.02.013, 2012.

Grewling, Ł., P. Bogawski, D. Jenerowicz, M. Czarnecka-Operacz, B. Šikoparija, C. A. Skjøth, and M. Smith, Mesoscale atmospheric transport of ragweed pollen allergens from infected to uninfected areas, *International Journal of Biometeorology*, doi:10.1007/s00484-016-1139-6, 2016.

Hamaoui-Laguel, L., R. Vautard, L. Liu, F. Solmon, N. Viovy, D. Khvorostyanov, F. Essl, I. Chuine, A. Colette, M. A. Semenov, A. Schaffhauser, J. Storkey, M. Thibaudon, and M. M. Epstein, Effects of climate change and seed dispersal on airborne ragweed pollen loads in Europe, *Nature Climate Change*, *5*(8), 766–771, doi:10.1038/nclimate2652, 2015.

Hänninen, O., A. B. Knol, M. Jantunen, T.-A. Lim, A. Conrad, M. Rappolder, P. Carrer, A.-C. Fanetti, R. Kim, J. Buekers, R. Torfs, I. Iavarone, T. Classen, C. Hornberg, and O. C. L. Mekel, Environmental Burden of Disease in Europe: Assessing Nine Risk Factors in Six Countries., *Environmental health perspectives*, *122*(5), 439–446, doi:10.1289/ehp.1206154, 2014.

Hansell, A. L., R. E. Ghosh, M. Blangiardo, C. Perkins, K. Vienneau, Danielle Goffe, D. Briggs, and J. Gulliver, Historic air pollution exposure and long-term mortality risks in England and Wales: Prospective longitudinal cohort study, *Thorax*, *In review*, 1–9, doi:10.1136/thoraxjnl-2015-207111, 2015.

Hass, H., P. J. H. Builtjes, D. Simpson, and R. Stern, Comparison of Model Results Obtained With Several European Regional Air Quality Models, *Atmospheric Environment*, *31*(19), 3259–3279, 1997.

Hass, H., M. van Loon, C. Kessler, R. Stern, J. Matthijsen, F. Sauter, Z. Zlatev, J. Langner, V. Voltescu, and M. Schaap, Aerosol modeling: results and intercomparison from European regional-scale modeling systems. A contribution to the EUROTRAC-2 subproject GLOREAM., *Tech. rep.*, EUROTRAC-2 subproject GLOREAM, 2003.

Helbig, N., B. Vogel, H. Vogel, and F. Fiedler, Numerical modelling of pollen dispersion on the regional scale, *Aerobiologia*, *3*, 3–19, 2004.

Hirst, J., An automatic volumetric spore trap, *The Annals of Applied Biology*, *39*(2), 257–265, 1952.

Hongisto, M., Impact of the emissions of international sea traffic on airborne deposition to the Baltic Sea and concentrations at the coastline, *Oceanologia*, *56*(2), 349–372, doi:10.5697/oc.56-2.349, 2014.

Hourdin, F., and O. Talagrand, Eulerian backtracking of atmospheric tracers. I: Adjoint derivation and parametrization of subgrid-scale transport, *Quarterly Journal of the Royal Meteorological Society*, *132*(615), 567–583, doi:10.1256/qj.03.198.A, 2006.

Huijnen, V., H. J. Eskes, A. Poupkou, H. Elbern, K. F. Boersma, G. Foret, M. Sofiev, A. Valdebenito, J. Flemming, O. Stein, A. Gross, L. Robertson, M. D'Isidoro, I. Kioutsioukis, E. Friese, B. Amstrup, R. Bergstrom, A. Strunk, J. Vira, D. Zyryanov, A. Maurizi, D. Melas, V.-H. Peuch, and C. Zerefos, Comparison of OMI NO2 tropospheric columns with an ensemble of global and European regional air quality models, *Atmospheric Chemistry and Physics*, *10*(7), 3273–3296, 2010a.

Huijnen, V., J. Williams, M. van Weele, T. van Noije, M. Krol, F. Dentener, A. Segers, S. Houweling, W. Peters, J. de Laat, F. Boersma, P. Bergamaschi, P. van Velthoven, P. Le Sager, H. Eskes, F. Alkemade, R. Scheele, P. Nédélec, and H.-W. Pätz, The global chemistry transport model TM5: description and evaluation of the tropospheric chemistry version 3.0, *Geoscientific Model Development*, *3*(2), 445–473, doi:10.5194/gmd-3-445-2010, 2010b.

Im, U., R. Bianconi, E. Solazzo, I. Kioutsioukis, A. Badia, A. Balzarini, R. Baró, R. Bellasio, D. Brunner, C. Chemel, G. Curci, H. Denier van der Gon, J. Flemming, R. Forkel, L. Giordano, P. Jiménez-Guerrero, M. Hirtl, A. Hodzic, L. Honzak, O. Jorba, C. Knote, P. A. Makar, A. Manders-Groot, L. Neal, J. L. Pérez, G. Pirovano, G. Pouliot, R. San Jose, N. Savage, W. Schroder, R. S. Sokhi, D. Syrakov, A. Torian, P. Tuccella, K. Wang, J. Werhahn, R. Wolke, R. Zabkar, Y. Zhang, J. Zhang, C. Hogrefe, and S. Galmarini, Evaluation of operational online-coupled regional air quality models over Europe and North America in the context of AQMEII phase 2. Part II: Particulate matter, *Atmospheric Environment*, doi:10.1016/j.atmosenv.2014.08.072, 2014.

IPCC, *Climate Change 2013: The Physical Science Basis. Contribution of Working Group I to the Fifth Assessment Report of the Intergovernmental Panel on Climate Change*, 1552 pp., Cambridge University Press, Cambridge, 2013.

Jing, B., S. R. Tong, Q. F. Liu, K. Li, W. G. Wang, Y. H. Zhang, and M. F. Ge, Hygroscopic behavior of multicomponent organic aerosols and their internal mixtures with ammonium sulfate, *Atmospheric Chemistry and Physics Discussions*, *15*, 23,357–23,405, doi:10.5194/acpd-15-23357-2015, 2015.

Kaiser, J. W., a. Heil, M. O. Andreae, a. Benedetti, N. Chubarova, L. Jones, J.-J. Morcrette, M. Razinger, M. G. Schultz, M. Suttie, and G. R. van der Werf, Biomass burning emissions estimated with a global fire assimilation system based on observed fire radiative power, *Biogeosciences*, *9*(1), 527–554, doi:10.5194/bg-9-527-2012, 2012.

Karrer, G., C. A. Skoth, B. Sikoparija, M. Smith, U. Berger, and F. Essl, Ragweed (Ambrosia) pollen source inventory for Austria, *Science of the Total Environment*, *523*, 120–128, doi:10.1016/j.scitotenv.2015.03.108, 2015.

Khain, A. P., Notes on state-of-the-art investigations of aerosol effects on precipitation: a critical review, *Environmental Research Letters*, *4*, 1–20, doi:10.1088/1748-9326/4/1/015004, 2009.

Kim, D., M. Chin, H. Yu, T. Diehl, Q. Tan, R. a. Kahn, K. Tsigaridis, S. E. Bauer, T. Takemura, L. Pozzoli, N. Bellouin, M. Schulz, S. Peyridieu, A. Chédin, and B. Koffi, Sources, sinks, and transatlantic transport of North African dust aerosol: A multimodel

analysis and comparison with remote sensing data, *Journal of Geophysical Research: Atmospheres*, pp. n/a–n/a, doi:10.1002/2013JD021099, 2014.

Kouznetsov, R., and M. Sofiev, A methodology for evaluation of vertical dispersion and dry deposition of atmospheric aerosols, *Journal of Geophysical Research*, *117*(D01202), doi:doi:10.1029/2011JD016366, 2012.

Kuenen, J. J. P., a. J. H. Visschedijk, M. Jozwicka, and H. a. C. Denier van der Gon, TNO-MACC_II emission inventory: a multi-year (2003-2009) consistent high-resolution European emission inventory for air quality modelling, *Atmospheric Chemistry and Physics Discussions*, *14*(5), 5837–5869, doi:10.5194/acpd-14-5837-2014, 2014.

Kukkonen, J., T. Olsson, D. M. Schultz, A. Baklanov, T. Klein, A. I. Miranda, A. Monteiro, M. Hirtl, V. Tarvainen, M. Boy, V.-H. Peuch, A. Poupkou, I. Kioutsioukis, S. Finardi, M. Sofiev, R. Sokhi, K. E. J. Lehtinen, K. Karatzas, R. San José, M. Astitha, G. Kallos, M. Schaap, E. Reimer, H. Jakobs, and K. Eben, A review of operational, regional-scale, chemical weather forecasting models in Europe, *Atmospheric Chemistry and Physics*, *12*(1), 1–87, doi:10.5194/acp-12-1-2012, 2012.

Lane, T. E., N. M. Donahue, and S. N. Pandis, Simulating secondary organic aerosol formation using the volatility basis-set approach in a chemical transport model, *Atmospheric Environment*, *42*(32), 7439–7451, doi:10.1016/j.atmosenv.2008.06.026, 2008.

Langner, J., M. Engardt, A. Baklanov, J. H. Christensen, M. Gauss, C. Geels, G. B. Hedegaard, R. Nuterman, D. Simpson, J. Soares, M. Sofiev, P. Wind, and A. Zakey, A multi-model study of impacts of climate change on surface ozone in Europe, *Atmospheric Chemistry and Physics*, *12*(21), 10,423–10,440, doi:10.5194/acp-12-10423-2012, 2012.

Larson, T., and J. Koenig, A summary of the emissions characterization and noncancer respiratory effects of wood smoke, *Tech. rep.*, US EPA, 1993.

Lee, D. S., R. D. Kingdon, J. M. Pacyna, A. F. Bouwman, and I. Tegen, Modelling base cations in Europe—sources, transport and deposition of calcium, *Atmospheric Environment*, *33*(14), 2241–2256, doi:http://dx.doi.org/10.1016/S1352-2310(98)00169-1, 1999.

Leiblein-Wild, M. C., J. Steinkamp, T. Hickler, and O. Tackenberg, Modelling the potential distribution, net primary production and phenology of common ragweed with a physiological model, *Journal of Biogeography*, pp. 544–554, doi:10.1111/jbi.12646, 2015.

Lim, S. S., T. Vos, A. D. Flaxman, G. Danaei, K. Shibuya, H. Adair-Rohani, M. Amann, H. R. Anderson, K. G. Andrews, M. Aryee, C. Atkinson, L. J. Bacchus, A. N. Bahalim, K. Balakrishnan, J. Balmes, S. Barker-Collo, A. Baxter, M. L. Bell, J. D. Blore, F. Blyth, C. Bonner, G. Borges, R. Bourne, M. Boussinesq, M. Brauer, P. Brooks, N. G. Bruce, B. Brunekreef, C. Bryan-Hancock, C. Bucello, R. Buchbinder, F. Bull, R. T. Burnett, T. E. Byers, B. Calabria, J. Carapetis, E. Carnahan, Z. Chafe, F. Charlson, H. Chen, J. S. Chen, A. T.-A. Cheng, J. C. Child, A. Cohen, K. E. Colson, B. C. Cowie, S. Darby, S. Darling, A. Davis, L. Degenhardt, F. Dentener, D. C. Des Jarlais, K. Devries, M. Dherani, E. L. Ding, E. R. Dorsey, T. Driscoll, K. Edmond, S. E. Ali, R. E. Engell, P. J. Erwin, S. Fahimi, G. Falder, F. Farzadfar, A. Ferrari, M. M. Finucane, S. Flaxman, F. G. R. Fowkes, G. Freedman, M. K. Freeman, E. Gakidou, S. Ghosh, E. Giovannucci, G. Gmel, K. Graham, R. Grainger, B. Grant, D. Gunnell, H. R. Gutierrez, W. Hall, H. W. Hoek, A. Hogan, H. D. Hosgood, D. Hoy, H. Hu, B. J. Hubbell, S. J.

Hutchings, S. E. Ibeanusi, G. L. Jacklyn, R. Jasrasaria, J. B. Jonas, H. Kan, J. A. Kanis, N. Kassebaum, N. Kawakami, Y.-H. Khang, S. Khatibzadeh, J.-P. Khoo, C. Kok, F. Laden, R. Lalloo, Q. Lan, T. Lathlean, J. L. Leasher, J. Leigh, Y. Li, J. K. Lin, S. E. Lipshultz, S. London, R. Lozano, Y. Lu, J. Mak, R. Malekzadeh, L. Mallinger, W. Marcenes, L. March, R. Marks, R. Martin, P. McGale, J. McGrath, S. Mehta, G. A. Mensah, T. R. Merriman, R. Micha, C. Michaud, V. Mishra, K. Mohd Hanafiah, A. A. Mokdad, L. Morawska, D. Mozaffarian, T. Murphy, M. Naghavi, B. Neal, P. K. Nelson, J. M. Nolla, R. Norman, C. Olives, S. B. Omer, J. Orchard, R. Osborne, B. Ostro, A. Page, K. D. Pandey, C. D. H. Parry, E. Passmore, J. Patra, N. Pearce, P. M. Pelizzari, M. Petzold, M. R. Phillips, D. Pope, C. A. Pope, J. Powles, M. Rao, H. Razavi, E. A. Rehfuess, J. T. Rehm, B. Ritz, F. P. Rivara, T. Roberts, C. Robinson, J. A. Rodriguez-Portales, I. Romieu, R. Room, L. C. Rosenfeld, A. Roy, L. Rushton, J. A. Salomon, U. Sampson, L. Sanchez-Riera, E. Sanman, A. Sapkota, S. Seedat, P. Shi, K. Shield, R. Shivakoti, G. M. Singh, D. A. Sleet, E. Smith, K. R. Smith, N. J. C. Stapelberg, K. Steenland, H. Stöckl, L. J. Stovner, K. Straif, L. Straney, G. D. Thurston, J. H. Tran, R. Van Dingenen, A. van Donkelaar, J. L. Veerman, L. Vijayakumar, R. Weintraub, M. M. Weissman, R. A. White, H. Whiteford, S. T. Wiersma, J. D. Wilkinson, H. C. Williams, W. Williams, N. Wilson, A. D. Woolf, P. Yip, J. M. Zielinski, A. D. Lopez, C. J. L. Murray, M. Ezzati, M. A. AlMazroa, and Z. A. Memish, A comparative risk assessment of burden of disease and injury attributable to 67 risk factors and risk factor clusters in 21 regions, 1990-2010: a systematic analysis for the Global Burden of Disease Study 2010., *Lancet*, *380*(9859), 2224–60, doi:10.1016/S0140-6736(12)61766-8, 2012.

Linkosalo, T., R. Häkkinen, and H. Hänninen, Models of the spring phenology of boreal and temperate trees: Is there something missing?, *Tree physiology*, *26*(9), 1165–1172, doi:10.1093/treephys/26.9.1165, 2006.

Loomis, D., Y. Grosse, B. Lauby-Secretan, F. E. Ghissassi, V. Bouvard, L. Benbrahim-Tallaa, N. Guha, R. Baan, H. Mattock, and K. Straif, The carcinogenicity of outdoor air pollution, *The Lancet Oncology*, *14*(13), 1262–1263, doi:10.1016/S1470-2045(13)70487-X, 2013.

Mahura, a., a. Baklanov, and U. Korsholm, Parameterization of the birch pollen diurnal cycle, *Aerobiologia*, *25*(4), 203–208, doi:10.1007/s10453-009-9125-7, 2009.

Marconi, M., D. M. Sferlazzo, S. Becagli, C. Bommarito, G. Calzolai, M. Chiari, a. Di Sarra, C. Ghedini, J. L. Gómez-Amo, F. Lucarelli, D. Meloni, F. Monteleone, S. Nava, G. Pace, S. Piacentino, F. Rugi, M. Severi, R. Traversi, and R. Udisti, Saharan dust aerosol over the central Mediterranean Sea: PM10 chemical composition and concentration versus optical columnar measurements, *Atmospheric Chemistry and Physics*, *14*, 2039–2054, doi:10.5194/acp-14-2039-2014, 2014.

Marécal, V., V.-H. Peuch, C. Andersson, S. Andersson, J. Arteta, M. Beekmann, a. Benedictow, R. Bergström, B. Bessagnet, a. Cansado, F. Chéroux, a. Colette, a. Coman, R. L. Curier, H. a. C. Denier van der Gon, a. Drouin, H. Elbern, E. Emili, R. J. Engelen, H. J. Eskes, G. Foret, E. Friese, M. Gauss, C. Giannaros, J. Guth, M. Joly, E. Jaumouillé, B. Josse, N. Kadygrov, J. W. Kaiser, K. Krajsek, J. Kuenen, U. Kumar, N. Liora, E. Lopez, L. Malherbe, I. Martinez, D. Melas, F. Meleux, L. Menut, P. Moinat, T. Morales, J. Parmentier, a. Piacentini, M. Plu, a. Poupkou, S. Queguiner, L. Robertson, L. Rouïl, M. Schaap, a. Segers, M. Sofiev, L. Tarasson, M. Thomas, R. Timmermans, Á. Valdebenito, P. van Velthoven, R. van Versendaal, J. Vira, and a. Ung, A re-

gional air quality forecasting system over Europe: the MACC-II daily ensemble production, *Geoscientific Model Development*, *8*(9), 2777–2813, doi:10.5194/gmd-8-2777-2015, 2015.

Mårtensson, E. M., E. D. Nilson, G. de Leeuw, L. H. Cohen, and H.-C. Hansson, Laboratory simulations and parameterization of the primary marine aerosol production, *Journal of Geophysical Research*, *108*(D9), 1–12, doi:10.1029/2002JD002263, 2003.

Martin, S. T., Phase Transitions of Aqueous Atmospheric Particles, *Chemical Reviews*, *100*(9), 3403–3454, doi:10.1021/cr990034t, 2000.

Matthias, V., A. Aulinger, and M. Quante, CMAQ simulations of the benzo(a)pyrene distribution over Europe for 2000 and 2001, *Atmospheric Environment*, *43*(26), 4078–4086, doi:10.1016/j.atmosenv.2009.04.058, 2009.

McLinden, C. A., V. Fioletov, M. W. Shephard, N. Krotkov, C. Li, R. V. Martin, M. D. Moran, and J. Joiner, Space-based detection of missing sulfur dioxide sources of global air pollution, *Nature Geoscience*, (May), 1–7, doi:10.1038/ngeo2724, 2016.

Monahan, E. C., D. E. Spiel, and K. L. Davidson, A model of marine aerosol generation via whitecaps and wave disruption, in *Oceanic whitecaps*, edited by E. C. Monahan and G. M. Niocell, pp. 167–174, D. Reidel Publishing, 1986.

Nenes, A., S. N. Pandis, and C. Pilinis, ISORROPIA: A new thermodynamic equilibrium model for multiphase multicomponent inorganic aerosols, *Aquatic Geochemistry*, *4*(1), 123–152, doi:10.1023/A:1009604003981, 1998.

Orlandi, F., H. Garcia-Mozo, L. V. Ezquerra, B. Romano, E. Dominguez, C. Galan, and M. Fornaciari, Phenological olive chilling requirements in Umbria (Italy) and Andalusia (Spain), *Plant Biosystems - An International Journal Dealing with all Aspects of Plant Biology*, *138*(2), 111–116, doi:10.1080/11263500412331283762, 2004.

Ostro, B., A. Tobias, X. Querol, A. Alastuey, F. Amato, J. Pey, N. Perez, and J. Sunyer, The effects of particulate matter sources on daily mortality: a case-crossover study of Barcelona, Spain., *Environmental health perspectives*, *119*(12), 1781–1787, doi:10.1289/ehp.1103618, 2011.

Ots, R., M. Vieno, J. D. Allan, S. Reis, E. Nemitz, D. E. Young, H. Coe, C. Di Marco, A. Detournay, I. A. Mackenzie, D. C. Green, and M. R. Heal, Model simulations of cooking organic aerosol (COA) over the UK using estimates of emissions based on measurements at two sites in London, *Atmospheric Chemistry and Physics Discussions*, (June), 1–28, doi:10.5194/acp-2016-342, 2016a.

Ots, R., D. E. Young, M. Vieno, L. Xu, R. E. Dunmore, J. D. Allan, H. Coe, L. R. Williams, S. C. Herndon, N. L. Ng, J. F. Hamilton, R. Bergström, C. Di Marco, E. Nemitz, I. A. Mackenzie11, J. J. P. Kuenen, D. C. Green, S. Reis, and M. R. Heal, Simulating secondary organic aerosol from missing diesel-related intermediate-volatility organic compound emissions during the Clean Air for London (ClearfLo) campaign, *Atmospheric Chemistry and Physics Discussions*, (in review), doi:10.5194/acp-2015-920, 2016b.

Päivinen, R., M. Lehikoinen, A. Schuck, T. Häme, S. Väätäinen, P. Kennedy, and S. Folving, Combining earth observation data and forest statistics, *Tech. rep.*, European Forest Institute, Joensuu, Finland, 2001.

Poupkou, A., T. Giannaros, K. Markakis, I. Kioutsioukis, G. Curci, D. Melas, and C. Zerefos, A model for European Biogenic Volatile Organic Compound emissions: Software development and first validation, *Environmental Modelling & Software*, *25*(12), 1845–1856, doi:10.1016/j.envsoft.2010.05.004, 2010.

Prank, M., M. Sofiev, P. Siljamo, M. Kauhaniemi, and European Aeroallergen Network, Increasing the Number of Allergenic Pollen Species in SILAM Forecasts, in *Air Pollution Modeling and its Application XXIV - Part of the series Springer Proceedings in Complexity*, edited by D. G. Steyn and N. Chaumerliac, pp. 313–317, Springer, doi:10.1007/978-3-319-24478-5_51, 2016.

Pudykiewicz, J. A., Application of adjoint tracer transport equations for evaluating source parameters, *Atmospheric Environment*, *32*(17), 3039–3050, doi:10.1016/S1352-2310(97)00480-9, 1998.

Putaud, J.-P., F. Raes, R. Van Dingenen, E. Brüggemann, M.-C. Facchini, S. Decesari, S. Fuzzi, R. Gehrig, C. Hüglin, P. Laj, G. Lorbeer, W. Maenhaut, N. Mihalopoulos, K. Müller, X. Querol, S. Rodriguez, J. Schneider, G. Spindler, H. T. Brink, K. Tørseth, and A. Wiedensohler, A European aerosol phenomenology-2: chemical characteristics of particulate matter at kerbside, urban, rural and background sites in Europe, *Atmospheric Environment*, *38*(16), 2579–2595, doi:10.1016/j.atmosenv.2004.01.041, 2004a.

Putaud, J.-P., R. Van Dingenen, A. Dell'Acqua, F. Raes, E. Matta, S. Decesari, M. C. Facchini, and S. Fuzzi, Size-segregated aerosol mass closure and chemical composition in Monte Cimone (I) during MINATROC, *Atmospheric Chemistry and Physics*, *4*, 889–902, doi:10.5194/acpd-3-4097-2003, 2004b.

Putaud, J.-P., R. Van Dingenen, A. Alastuey, H. Bauer, W. Birmili, J. Cyrys, H. Flentje, S. Fuzzi, R. Gehrig, H. Hansson, R. Harrison, H. Herrmann, R. Hitzenberger, C. Hüglin, A. Jones, A. Kasper-Giebl, G. Kiss, A. Kousa, T. Kuhlbusch, G. Löschau, W. Maenhaut, A. Molnar, T. Moreno, J. Pekkanen, C. Perrino, M. Pitz, H. Puxbaum, X. Querol, S. Rodriguez, I. Salma, J. Schwarz, J. Smolik, J. Schneider, G. Spindler, H. ten Brink, J. Tursic, M. Viana, A. Wiedensohler, and F. Raes, A European aerosol phenomenology - 3: Physical and chemical characteristics of particulate matter from 60 rural, urban, and kerbside sites across Europe, *Atmospheric Environment*, *44*(10), 1308–1320, doi:10.1016/j.atmosenv.2009.12.011, 2010.

Rao, S. T., S. Galmarini, and K. Puckett, Air quality model evaluation international initiative (AQMEII): Advancing the state of the science in regional photochemical modeling and its applications, *Bulletin of the American Meteorological Society*, *92*(1), 23–30, doi:10.1175/2010BAMS3069.1, 2011.

Robinson, A. L., N. M. Donahue, M. K. Shrivastava, E. a. Weitkamp, A. M. Sage, A. P. Grieshop, T. E. Lane, J. R. Pierce, and S. N. Pandis, Rethinking Organic Aerosols : Semivolatile Emissions and Photochemical Aging, *Science*, *315*, 1259–1262, doi:10.1126/science.1133061, 2007.

Rohr, A. C., and R. E. Wyzga, Attributing health effects to individual particulate matter constituents, *Atmospheric Environment*, *62*, 130–152, doi:10.1016/j.atmosenv.2012.07.036, 2012.

Schaap, M., Timmermans, R. M. A., M. Roemer, G. A. C. Boersen, P. J. H. Builtjes, F. J. Sauter, G. J. M. Velders, and J. P. Beck, The LOTOS-EUROS model: Description,

validation and latest developments, *international journal of environment and pollution*, *32*, 270–290, 2008.

Schlesinger, R. B., The Health Impact of Common Inorganic Components of Fine Particulate Matter (PM 2.5) in Ambient Air: A Critical Review, *Inhalation Toxicology*, *19*(10), 811–832, doi:10.1080/08958370701402382, 2007.

Schlesinger, R. B., and F. Cassee, Atmospheric secondary inorganic particulate matter: the toxicological perspective as a basis for health effects risk assessment, *Inhalation Toxicology*, *15*, 197–235, doi:10.1080/08958370390168247, 2003.

Schuck, A., J. Van Brusselen, R. Päivinen, T. Häme, P. Kennedy, and S. Folving, Compilation of a Calibrated European Forest Map Derived from NOAA-AVHRR Data, *Tech. rep.*, European Forest Institute, Joensuu, 2002.

Schueler, S., and K. H. Schlünzen, Modeling of oak pollen dispersal on the landscape level with a mesoscale atmospheric model, *Environmental Modeling and Assessment*, *11*(3), 179–194, doi:10.1007/s10666-006-9044-8, 2006.

Schueler, S., K. H. Schlünzen, and F. Scholz, Viability and sunlight sensitivity of oak pollen and its implications for pollen-mediated gene flow, *Trees - Structure and Function*, *19*(2), 154–161, doi:10.1007/s00468-004-0376-1, 2005.

Seinfeld, J. H., and S. N. Pandis, *Atmospheric chemistry and physics. From air pollution to climate change*, 2 ed., John Wiley & sons, Inc, Hoboken, New Jersey, 2006.

Shankar Rao, K., Source estimation methods for atmospheric dispersion, *Atmospheric Environment*, *41*(33), 6964–6973, doi:10.1016/j.atmosenv.2007.04.064, 2007.

Shrivastava, M., J. Fast, R. Easter, W. I. Gustafson, R. a. Zaveri, J. L. Jimenez, P. Saide, and A. Hodzic, Modeling organic aerosols in a megacity: Comparison of simple and complex representations of the volatility basis set approach, *Atmospheric Chemistry and Physics*, *11*(13), 6639–6662, doi:10.5194/acp-11-6639-2011, 2011.

Shrivastava, M. K., T. E. Lane, N. M. Donahue, S. N. Pandis, and A. L. Robinson, Effects of gas particle partitioning and aging of primary emissions on urban and regional organic aerosol concentrations, *Journal of Geophysical Research Atmospheres*, *113*(18), 1–16, doi:10.1029/2007JD009735, 2008.

Siljamo, P., M. Sofiev, E. Severova, H. Ranta, J. Kukkonen, S. Polevova, E. Kubin, and A. Minin, Sources, impact and exchange of early-spring birch pollen in the Moscow region and Finland, *Aerobiologia*, *24*(4), 211–230, doi:10.1007/s10453-008-9100-8, 2008.

Siljamo, P., M. Sofiev, E. Filatova, L. Grewling, S. Jäger, E. Khoreva, T. Linkosalo, S. Ortega Jimenez, H. Ranta, A. Rantio-Lehtimäki, A. Svetlov, L. Veriankaite, E. Yakovleva, and J. Kukkonen, A numerical model of birch pollen emission and dispersion in the atmosphere. Model evaluation and sensitivity analysis, *International journal of biometeorology*, *57*, 125–136, doi:10.1007/s00484-012-0539-5, 2013.

Sillanpää, M., R. Hillamo, S. Saarikoski, A. Frey, A. Pennanen, U. Makkonen, Z. Spolnik, R. Van Grieken, M. Braniš, and B. Brunekreef, Chemical composition and mass closure of particulate matter at six urban sites in Europe, *Atmospheric Environment*, *40*, 212–223, doi:10.1016/j.atmosenv.2006.01.063, 2006.

Simpson, D., A. Benedictow, H. Berge, R. Bergström, L. D. Emberson, H. Fagerli, C. R. Flechard, G. D. Hayman, M. Gauss, J. E. Jonson, M. E. Jenkin, A. Nyíri, C. Richter, V. S. Semeena, S. Tsyro, J.-P. Tuovinen, Á. Valdebenito, and P. Wind, The EMEP MSC-W chemical transport model - technical description, *Atmospheric Chemistry and Physics*, *12*(16), 7825–7865, doi:10.5194/acp-12-7825-2012, 2012.

Simpson, D., C. Andersson, J. H. Christensen, M. Engardt, C. Geels, A. Nyiri, M. Posch, J. Soares, M. Sofiev, P. Wind, and J. Langner, Impacts of climate and emission changes on nitrogen deposition in Europe : a multi-model study, *Atmospheric Chemistry and Physics*, *14*, 6663–6720, doi:10.5194/acpd-14-6663-2014, 2014.

Skjøth, C. A., M. Smith, B. Šikoparija, A. Stach, D. Myszkowska, I. Kasprzyk, P. Radišić, B. Stjepanović, I. Hrga, and D. Apatini, A method for producing airborne pollen source inventories: An example of Ambrosia (ragweed) on the Pannonian Plain, *Agricultural and Forest Meteorology*, *150*(9), 1203–1210, doi:10.1016/j.agrformet.2010.05.002, 2010.

Soares, J., M. Sofiev, and J. Hakkarainen, Uncertainties of wild-land fires emission in AQMEII phase 2 case study, *Atmospheric Environment*, doi:10.1016/j.atmosenv.2015.01.068, 2015.

Soares, J., M. Sofiev, C. Geels, J. H. Christensen, C. Andersson, S. Tsyro, and J. Langner, Impact of climate change on the production and transport of sea salt aerosol on European seas, *Atmospheric Chemistry and Physics Discussions*, (February), 1–52, doi:10.5194/acp-2015-1056, 2016.

Sofiev, M., A model for the evaluation of long-term airborne pollution transport at regional and continental scales, *Atmospheric Environment*, *34*(15), 2481–2493, doi:10.1016/S1352-2310(99)00415-X, 2000.

Sofiev, M., and K.-C. Bergmann (Eds.), *Allergenic Pollen: A Review of the Production, Release, Distribution and Health Impacts*, 247 pp., Springer, Dordrecht, doi:10.1007/978-94-007-4881-1, 2013.

Sofiev, M., P. Siljamo, H. Ranta, and A. Rantio-Lehtimäki, Towards numerical forecasting of long-range air transport of birch pollen: theoretical considerations and a feasibility study., *International journal of biometeorology*, *50*(6), 392–402, doi:10.1007/s00484-006-0027-x, 2006a.

Sofiev, M., P. Siljamo, I. Valkama, M. Ilvonen, and J. Kukkonen, A dispersion modelling system SILAM and its evaluation against ETEX data, *Atmospheric Environment*, *40*(4), 674–685, doi:10.1016/j.atmosenv.2005.09.069, 2006b.

Sofiev, M., R. Vankevich, M. Lotjonen, M. Prank, V. Petukhov, T. Ermakova, J. Koskinen, and J. Kukkonen, An operational system for the assimilation of the satellite information on wild-land fires for the needs of air quality modelling and forecasting, *Atmospheric Chemistry and Physics*, *9*(18), 6833–6847, doi:10.5194/acpd-9-6483-2009, 2009.

Sofiev, M., E. Genikhovich, P. Keronen, and T. Vesala, Diagnosing the Surface Layer Parameters for Dispersion Models within the Meteorological-to-Dispersion Modeling Interface, *Journal of Applied Meteorology and Climatology*, *49*(2), 221–233, doi:10.1175/2009JAMC2210.1, 2010.

Sofiev, M., J. Soares, M. Prank, G. de Leeuw, and J. Kukkonen, A regional-to-global model of emission and transport of sea salt particles in the atmosphere, *Journal of Geophysical Research*, *116*(D21302), 25, doi:10.1029/2010JD014713, 2011.

Sofiev, M., T. Ermakova, and R. Vankevich, Evaluation of the smoke-injection height from wild-land fires using remote-sensing data, *Atmospheric Chemistry and Physics*, *12*(4), 1995–2006, doi:10.5194/acp-12-1995-2012, 2012.

Sofiev, M., R. Vankevich, T. Ermakova, and J. Hakkarainen, Global mapping of maximum emission heights and resulting vertical profiles of wildfire emissions, *Atmospheric Chemistry and Physics*, *13*(14), 7039–7052, doi:10.5194/acp-13-7039-2013, 2013.

Sofiev, M., U. Berger, M. Prank, J. Vira, J. Arteta, J. Belmonte, K. C. Bergmann, F. Cheroux, H. Elbern, E. Friese, C. Galan, R. Gehrig, D. Khvorostyanov, R. Kranenburg, U. Kumar, Mare, V. Cal, F. Meleux, L. Menut, A. M. Pessi, L. Robertson, O. Ritenberga, V. Rodinkova, A. Saarto, A. Segers, E. Severova, I. Sauliene, P. Siljamo, B. M. Steensen, E. Teinemaa, M. Thibaudon, and V. H. Peuch, MACC regional multi-model ensemble simulations of birch pollen dispersion in Europe, *Atmospheric Chemistry and Physics*, *15*(14), 8115–8130, doi:10.5194/acp-15-8115-2015, 2015a.

Sofiev, M., J. Vira, R. Kouznetsov, M. Prank, J. Soares, and E. Genikhovich, Construction of an Eulerian atmospheric dispersion model based on the advection algorithm of M. Galperin: dynamic cores v.4 and 5 of SILAM v.5.5, *Geoscientific Model Development Discussions*, *8*(1), 1–43, doi:10.5194/gmdd-8-1-2015, 2015b.

Solazzo, E., R. Bianconi, G. Pirovano, V. Matthias, R. Vautard, M. D. Moran, K. Wyat Appel, B. Bessagnet, J. Brandt, J. H. Christensen, C. Chemel, I. Coll, J. Ferreira, R. Forkel, X. V. Francis, G. Grell, P. Grossi, A. B. Hansen, A. I. Miranda, U. Nopmongcol, M. Prank, K. N. Sartelet, M. Schaap, J. D. Silver, R. S. Sokhi, J. Vira, J. Werhahn, R. Wolke, G. Yarwood, J. Zhang, S. T. Rao, and S. Galmarini, Operational model evaluation for particulate matter in Europe and North America in the context of AQMEII, *Atmospheric Environment*, *53*, 75–92, doi:10.1016/j.atmosenv.2012.02.045, 2012a.

Solazzo, E., R. Bianconi, R. Vautard, K. W. Appel, M. D. Moran, C. Hogrefe, B. Bessagnet, J. Brandt, J. H. Christensen, C. Chemel, I. Coll, H. Denier van der Gon, J. Ferreira, R. Forkel, X. V. Francis, G. Grell, P. Grossi, A. B. Hansen, A. Jeričević, L. Kraljević, A. I. Miranda, U. Nopmongcol, G. Pirovano, M. Prank, A. Riccio, K. N. Sartelet, M. Schaap, J. D. Silver, R. S. Sokhi, J. Vira, J. Werhahn, R. Wolke, G. Yarwood, J. Zhang, S. Rao, and S. Galmarini, Model evaluation and ensemble modelling of surface-level ozone in Europe and North America in the context of AQMEII, *Atmospheric Environment*, *53*, 60–74, doi:10.1016/j.atmosenv.2012.01.003, 2012b.

Solazzo, E., R. Bianconi, G. Pirovano, M. D. Moran, R. Vautard, C. Hogrefe, K. W. Appel, V. Matthias, P. Grossi, B. Bessagnet, J. Brandt, C. Chemel, J. H. Christensen, R. Forkel, X. V. Francis, A. B. Hansen, S. McKeen, U. Nopmongco, M. Prank, K. N. Sartelet, A. Segers, J. D. Silver, G. Yarwood, J.Werhahn, J.Zhang, S. T. Rao, and S. Galmarini, Evaluating the capability of regional-scale air quality models to capture the vertical distribution of pollutants, *Geosci. Model Dev*, *6*, 791–818, doi:10.5194/gmd-6-791-2013, 2013.

Spicer, C. W., E. G. Chapman, B. J. Finlayson-Pitts, R. A. Plastridge, J. M. Hubbe, J. D. Fast, and C. M. Berkowitz, Unexpectedly high concentrations of molecular chlorine in coastal air, *Nature*, *394*(6691), 353–356, doi:10.1038/28584, 1998.

Spieksma, F. T. M., G. Frenguelli, a. H. Nikkels, G. Mincigrucci, L. O. M. J. Smithuis, E. Bricchi, W. Dankaart, and B. Romano, Comparative study of airborne pollen concentrations in central Italy and the Netherlands (1982-1985), *Grana*, *28*(1), 25–36, doi:10.1080/00173138909431009, 1989.

Stanek, L. W., J. D. Sacks, S. J. Dutton, and J.-J. B. Dubois, Attributing health effects to apportioned components and sources of particulate matter: An evaluation of collective results, *Atmospheric Environment*, *45*(32), 5655–5663, doi:10.1016/j.atmosenv.2011.07.023, 2011.

Stein, A., R. Draxler, G. Rolph, B. Stunder, M. Cohen, and F. Ngan, NOAA's HYSPLIT atmospheric transport and dispersion modeling system, *Bulletin of the American Meteorological Society*, (February), 150504130527,006, doi:10.1175/BAMS-D-14-00110.1, 2015.

Stern, R., P. Builtjes, M. Schaap, R. Timmermans, R. Vautard, a. Hodzic, M. Memmesheimer, H. Feldmann, E. Renner, and R. Wolke, A model inter-comparison study focussing on episodes with elevated PM10 concentrations, *Atmospheric Environment*, *42*(19), 4567–4588, doi:10.1016/j.atmosenv.2008.01.068, 2008.

Stohl, A., S. Eckhardt, C. Forster, P. James, N. Spichtinger, and P. Seibert, A replacement for simple back trajectory calculations in the interpretation of atmospheric trace substance measurements, *Atmospheric Environment*, *36*(29), 4635–4648, doi:10.1016/S1352-2310(02)00416-8, 2002.

Storkey, J., P. Stratonovitch, D. S. Chapman, F. Vidotto, and M. A. Semenov, A process-based approach to predicting the effect of climate change on the distribution of an invasive allergenic plant in Europe, *PLoS ONE*, *9*(2), 1–7, doi:10.1371/journal.pone.0088156, 2014.

Taramarcaz, P., C. Lambelet, B. Clot, C. Keimer, and C. Hauser, Ragweed (Ambrosia) progression and its health risks : will Switzerland resist this invasion ?, *Swiss Medical Weekly*, *135*, 538–549, 2005.

Textor, C., M. Schulz, S. Guibert, S. Kinne, Y. Balkanski, S. Bauer, T. Berntsen, T. Berglen, O. Boucher, M. Chin, F. Dentener, T. Diehl, R. Easter, H. Feichter, D. Fillmore, S. Ghan, P. Ginoux, S. Gong, A. Grini, J. Hendricks, L. Horowitz, P. Huang, I. Isaksen, I. Iversen, S. Kloster, D. Koch, A. Kirkevåg, J. E. Kristjansson, M. Krol, A. Lauer, J. F. Lamarque, X. Liu, V. Montanaro, G. Myhre, J. Penner, G. Pitari, S. Reddy, Ø. Seland, P. Stier, T. Takemura, and X. Tie, Analysis and quantification of the diversities of aerosol life cycles within AeroCom, *Atmospheric Chemistry and Physics*, *6*, 1777–1813, 2006.

Thibaudon, M., B. Šikoparija, G. Oliver, M. Smith, and C. A. Skjøth, Ragweed pollen source inventory for France - The second largest centre of Ambrosia in Europe, *Atmospheric Environment*, *83*, 62–71, doi:10.1016/j.atmosenv.2013.10.057, 2014.

Trombik, J., and T. Hlásny, Free European data on forest distribution: Overview and evaluation, *Journal of Forest Science*, *59*(11), 447–457, 2013.

Tsyro, S., To what extent can aerosol water explain the discrepancy between model calculated and gravimetric PM 10 and PM 2.5?, *Atmospheric Chemistry and Physics*, *5*, 515–532, 2005.

Tsyro, S., W. Aas, J. Soares, M. Sofiev, H. Berge, and G. Spindler, Modelling of sea salt concentrations over Europe: Key uncertainties and comparison with observations, *Atmospheric Chemistry and Physics*, *11*(20), 10,367–10,388, doi:10.5194/acp-11-10367-2011, 2011.

Turpin, B. J., and H.-J. Lim, Species Contributions to PM2.5 Mass Concentrations: Revisiting Common Assumptions for Estimating Organic Mass, *Aerosol Science and Technology*, *35*(1), 602–610, doi:10.1080/02786820119445, 2001.

van der Werf, G. R., J. T. Randerson, L. Giglio, G. J. Collatz, M. Mu, P. S. Kasibhatla, D. C. Morton, R. S. DeFries, Y. Jin, and T. T. van Leeuwen, Global fire emissions and the contribution of deforestation, savanna, forest, agricultural, and peat fires (1997–2009), *Atmospheric Chemistry and Physics*, *10*(23), 11,707–11,735, doi:10.5194/acp-10-11707-2010, 2010.

Van Dingenen, R., F. Raes, J.-P. Putaud, U. Baltensperger, A. Charron, M.-C. Facchini, S. Decesari, S. Fuzzi, R. Gehrig, H.-C. Hansson, R. M. Harrison, C. Hüglin, A. M. Jones, P. Laj, G. Lorbeer, W. Maenhaut, F. Palmgren, X. Querol, S. Rodriguez, J. Schneider, H. T. Brink, P. Tunved, K. Tørseth, B. Wehner, E. Weingartner, A. Wiedensohler, and P. Wåhlin, A European aerosol phenomenology-1: physical characteristics of particulate matter at kerbside, urban, rural and background sites in Europe, *Atmospheric Environment*, *38*(16), 2561–2577, doi:10.1016/j.atmosenv.2004.01.040, 2004.

van Loon, M., L. Tarrasson, and M. Posch, Modelling Base Cations in Europe, *Tech. rep.*, Norwegian Meteorological Institute, 2005.

Vautard, R., P. H. J. Builtjes, P. Thunis, C. Cuvelier, M. Bedogni, B. Bessagnet, C. Honoré, N. Moussiopoulos, G. Pirovano, M. Schaap, R. Stern, L. Tarrason, and P. Wind, Evaluation and intercomparison of Ozone and PM10 simulations by several chemistry transport models over four European cities within the CityDelta project, *Atmospheric Environment*, *41*(1), 173–188, doi:10.1016/j.atmosenv.2006.07.039, 2007.

Vautard, R., M. Schaap, R. Bergström, B. Bessagnet, J. Brandt, P. Builtjes, J. Christensen, C. Cuvelier, V. Foltescu, and a. Graff, Skill and uncertainty of a regional air quality model ensemble, *Atmospheric Environment*, *43*(31), 4822–4832, doi:10.1016/j.atmosenv.2008.09.083, 2009.

Vira, J., and M. Sofiev, On variational data assimilation for estimating the model initial conditions and emission fluxes for short-term forecasting of SOx concentrations, *Atmospheric Environment*, *46*, 318–328, doi:10.1016/j.atmosenv.2011.09.066, 2012.

Visschedijk, A., P. Zandveld, H. D. V. D. Gon, T. European, C. For, M.-r. W. Forecasts, S. Park, and U. Kingdom, A high resolution gridded European emission database for the, *Tech. rep.*, TNO, Apeldoorn, 2007.

Vogel, H., A. Pauling, and B. Vogel, Numerical simulation of birch pollen dispersion with an operational weather forecast system, *International Journal of Biometeorology*, *52*(8), 805–814, doi:10.1007/s00484-008-0174-3, 2008.

Wichink Kruit, R., M. Schaap, F. Sauter, E. Van der Swaluw, and E. Weijers, Improving the understanding of the secondary inorganic aerosol distribution over the Netherlands, *Tech. rep.*, TNO report TNO-060-UT-2012-00334, Utrecht, 2012.

Yarwood, G., S. Rao, M. Yocke, and G. Whitten, Updates to the carbon bond chemical mechanism: CB05. Final Report, *Tech. rep.*, RT-04-00675, U.S. EPA, 2005.

Young, D. E., J. D. Allan, P. I. Williams, D. C. Green, M. J. Flynn, R. M. Harrison, J. Yin, M. W. Gallagher, and H. Coe, Investigating the annual behaviour of submicron secondary inorganic and organic aerosols in London, *Atmospheric Chemistry and Physics*, *15*, 6315–6366, doi:10.5194/acpd-14-18739-2014, 2015.

Zanobetti, A., and J. Schwartz, The effect of fine and coarse particulate air pollution on mortality: A national analysis, *Environmental Health Perspectives*, *117*(6), 898–903, doi:10.1289/ehp.0800108, 2009.

Zanobetti, A., E. Austin, B. A. Coull, J. Schwartz, and P. Koutrakis, Health effects of multi-pollutant profiles, *Environment International*, *71*, 13–19, doi:10.1016/j.envint.2014.05.023, 2014.

Zhang, R., T. Duhl, M. T. Salam, J. M. House, R. C. Flagan, E. L. Avol, F. D. Gilliland, a. Guenther, S. H. Chung, B. K. Lamb, and T. M. VanReken, Development of a regional-scale pollen emission and transport modeling framework for investigating the impact of climate change on allergic airway disease, *Biogeosciences*, *11*(6), 1461–1478, doi:10.5194/bg-11-1461-2014, 2014.

Zink, K., H. Vogel, B. Vogel, D. Magyar, and C. Kottmeier, Modeling the dispersion of Ambrosia artemisiifolia L. pollen with the model system COSMO-ART., *International journal of biometeorology*, *56*(4), 669–80, doi:10.1007/s00484-011-0468-8, 2012.

FINNISH METEOROLOGICAL INSTITUTE
Erik Palménin aukio 1
P.O. Box 503
FI-00101 HELSINKI
tel. +358 29 539 1000
WWW.FMI.FI

FINNISH METEOROLOGICAL INSTITUTE
CONTRIBUTIONS No. 128
ISBN 978-952-336-004-4 (paperback)
ISSN 0782-6117
Erweko
Helsinki 2016

ISBN 978-952-336-005-1 (pdf)
Helsinki 2016